

2016

## Modeling Churn and Annular Flow Regimes in Vertical and Near-Vertical Pipes with Small and Large Diameters

Erika Viana Pagan

*Louisiana State University and Agricultural and Mechanical College*

Follow this and additional works at: [https://digitalcommons.lsu.edu/gradschool\\_theses](https://digitalcommons.lsu.edu/gradschool_theses)



Part of the [Petroleum Engineering Commons](#)

---

### Recommended Citation

Viana Pagan, Erika, "Modeling Churn and Annular Flow Regimes in Vertical and Near-Vertical Pipes with Small and Large Diameters" (2016). *LSU Master's Theses*. 1140.

[https://digitalcommons.lsu.edu/gradschool\\_theses/1140](https://digitalcommons.lsu.edu/gradschool_theses/1140)

This Thesis is brought to you for free and open access by the Graduate School at LSU Digital Commons. It has been accepted for inclusion in LSU Master's Theses by an authorized graduate school editor of LSU Digital Commons. For more information, please contact [gradetd@lsu.edu](mailto:gradetd@lsu.edu).

# MODELING CHURN AND ANNULAR FLOW REGIMES IN VERTICAL AND NEAR-VERTICAL PIPES WITH SMALL AND LARGE DIAMETERS

A Thesis

Submitted to the Graduate Faculty of the  
Louisiana State University and  
Agricultural and Mechanical College  
in partial fulfillment of the  
requirements for the degree of  
Master of Science in Petroleum Engineering

in

The Department of Petroleum Engineering

by  
Erika Viana Pagan  
B.S., Universidade Federal do Ceará, 2011  
August 2016

## **Acknowledgements**

I would like to thank Louisiana State University for funding this research. I sincerely thank my supervisor Professor Paulo Waltrich for his mentoring, support, and patience throughout the duration of this study. His guidance and support have been profoundly valuable to me. I extend my gratitude to Professor Wesley Williams and Professor Seung Kam for helping me on the development of this research and for all the helpful and indispensable assistance when it was necessary.

Special thanks go to my husband Renato Coutinho for believing in my potential and for having always encouraged me to face new challenges, and helping on my personal and professional growth. I also acknowledge the support and care of my entire family, especially to my mother Maria das Dores Viana Pagan and my grandmother Elza Coelho, my brother Filipe Pagan, and my father Jose Carlos Pagan who stayed in my mother country, but have always been tracking my path, always hoping for new and great achievements in my life.

I also would like to express my gratitude to Pedro Sousa for sharing with me some of his knowledge and experience. Very special thanks to Matheus Pareto, Bruno Xavier, and Felipe Maciel for assistance getting some experimental data for this research and also for the assistance on implementing the model and running some of the simulations.

I am thankful to the faculty and staff of the Petroleum Engineering department who were essential to my learning process. I am also grateful to all the friends I conquered during my Master studies from the LSU Petroleum Engineering Department as well as from outside of school for helping this experience to be even more enjoyable.

## Table of Contents

Acknowledgements.....	ii
List of Tables .....	v
List of Figures .....	vi
Abstract.....	viii
1. Introduction .....	1
1.1 Flow Regimes.....	2
1.2 Two-Phase Flow Modeling in Small and Large Diameter Pipes .....	5
1.3 Objectives.....	6
1.4 Thesis Outline.....	7
2. Literature Review .....	9
2.1 Two-Phase Flow Modeling .....	9
2.1.1 Liquid Holdup.....	9
2.1.2 Pressure Gradient.....	10
2.1.2.1 Superficial Velocities.....	12
2.1.3 Annular Flow .....	13
2.1.4 Churn Flow .....	13
2.1.5 Correlations Available in the Literature .....	15
2.1.5.1 Duns and Ros (1963) Correlation .....	16
2.1.5.2 Gray (1974) Correlation.....	16
2.1.5.3 Ansari et al. (1994) Correlation .....	17
2.1.5.4 OLGA (2000) Correlation.....	17
2.2 Liquid Loading .....	18
2.2.1 Turner et al. (1969) Droplet Model.....	18
2.2.2 Minimum Pressure Point and Nodal Analysis .....	19
2.2.3 Coupled Reservoir/Wellbore Modeling.....	20
3. Models Description .....	23
3.1 Churn and Annular Flow Modeling .....	23
3.1.1 Momentum Equations.....	23
3.1.2 Wall and Interfacial Shear Stress.....	25
3.1.3 The Churn to Annular Flow Transition .....	28
3.1.4 The Slug/Bubble to Churn Flow Transition .....	28
3.1.5 Main Contributions of Proposed Model .....	30
3.2 Liquid Loading Initiation Model .....	31
3.2.1 Reservoir Inflow Performance Model (IPR).....	34
3.2.2 Tubing Performance Relationship (TPR) .....	34
4. Model Validation, Results and Discussions .....	38
4.1 Churn and Annular Flow Modeling Validation Results.....	38
4.1.1 Comparison with Laboratorial Data.....	39

4.1.2 Comparison with Field Data .....	46
4.2 Liquid Loading Modeling Validation and Result Discussions .....	51
4.2.1 Testing the Concept of Minimum Pressure Point and Nodal Analysis (Lea et al., 2003) with Field Data of Veeken et al. (2010) .....	58
4.2.2 Explaining Liquid Loading Field Symptoms Using the Proposed Model .....	59
5. Conclusions and Recommendations for Future Work .....	66
5.1 Conclusions on the Churn and Annular Flow Modeling .....	66
5.2 Conclusions on Liquid Loading Modeling .....	68
References .....	71
Appendix: Permissions to Publish Previously Published Works .....	77
Vita .....	82

## **List of Tables**

Table 1 – Liquid loading data set for vertical and near-vertical gas wells published by Veeken et al. (2010).....	53
---	----

## List of Figures

Figure 1.1 – Flow regimes for gas-liquid upwards flow in vertical pipes (Hewitt, 1982).....	3
Figure 2.1 – Graphical representation of the total pressure gradient for gas-liquid flow in vertical- or near-vertical pipes (Modified after Shoham, 2006). .....	11
Figure 2.2 - A schematic representation of distribution of phases and mass transfer mechanisms for (a) annular flow and (b) churn flow. These representations are based on experimental observations of Waltrich et al. (2013), using a clear vertical pipe (42 m long, and 0.048 m internal pipe diameter). .....	14
Figure 2.3 – The nodal analysis technique used to predict liquid loading in gas wells. The intersection between the IPR and TPR curves to left of the minimum pressure point defines if the well is under liquid loading conditions (Lea et al., 2003). .....	20
Figure 3.1 - Force balance for a pipe segment for churn and annular flow regimes on (a) gas core and (b) total cross-sectional area (including liquid film and gas core).....	24
Figure 3.2 – Proposed nodal analysis technique to predict liquid loading: (a) the tangent between the IPR and TPR curves defines liquid loading initiation, and (b) gas production rate suddenly declines after time $t_4$ as the reservoir cannot sustain steady-state two-phase flow for flow rates lower than $Q_{min}$ . .....	32
Figure 4.1 - Comparison between model and experimental results in terms of pressure gradient and liquid holdup (data from Skopich et al., 2015), for 0.0508 m (2 in) pipe diameter and superficial liquid velocities of (a) 0.01 m/s, and (b) 0.05 m/s. ....	40
Figure 4.2 - Comparison between model and experimental results in terms of pressure gradient and liquid holdup (data from Skopich et al., 2015), for 0.102 m (4 in) pipe diameter and superficial liquid velocities of (a) 0.01 m/s and (b) 0.05 m/s. ....	42
Figure 4.3 - Comparison between model and experimental results in terms of pressure gradient (data from Van de Meulen, 2012), for 0.127 m (5 in) pipe ID, and liquid superficial velocities of (a) 0.02 m/s and (b) 0.7 m/s. ....	43
Figure 4.4 - Comparison between model and experiments results in terms of pressure gradient (data from Zabararas et al., 2013) for 0.279 m (11 in) pipe ID, and liquid superficial velocities of (a) 0.03 m/s and (b) 0.15 m/s. ....	44
Figure 4.5 – (a) Absolute average error and (b) comparison between experimental and calculated pressure gradient for models used in this study. ....	45
Figure 4.6 – (a) Absolute average error, and (b) calculated and measured bottomhole pressure for the field database of Reinicke et al. (1987), for wells having tubing diameters around 0.101 m (3.976 in).....	47

Figure 4.7 - Comparison between simulation results using the model proposed in this study and measured wellbore pressure profile (field data from Fancher and Brown, 1963). Circles represent the measured pressures and continuous lines are the simulated pressures. Dash lines represents the depth at which a flow regime transition happened based on the simulation.....	49
Figure 4.8 - (a) Absolute average error, and (b) calculated and measured bottomhole pressure for the field database of Fancher and Brown (1963), for wells having tubing diameters around 0.0508 m (2 in).....	50
Figure 4.9 – Example on how Veeken et al. (2010) have defined the minimum gas flow ( $Q_{min}$ ) that represents the liquid loading initiation.....	52
Figure 4.10 – Examples on how the method of using IPR tangent to TPR curve was validated with the minimum production flow rate for wells: (a) 28a, (b) 28b in Veeken et al. (2010) database. The figure also shows the results for the prediction of liquid loading initiation using the droplet model of Turner et al. (1969).....	54
Figure 4.11 – (a) Relative error, and (b) absolute average error for the comparison between field data published by Veeken et al. (2010) for the predicted minimum flow rate for liquid loading initiation. These results show the prediction for the field data using the concept of IPR tangent to the TPR proposed, using TPR model proposed in this study and Gray (1974). Turner et al. (1969) critical flow rate is also compared to the same field data set. The angle ( $\theta$ ) above the x-axis in figure (a) indicates the inclination of the well. ....	56
Figure 4.12 – (a) Relative error and (b) absolute average error for the comparison between field data published by Veeken et al. (2010) for the predicted minimum flow rate for liquid loading initiation when using the concept of minimum pressure of Lea et al. (2003) with the TPR model proposed in this study and Gray (1974). Figure 4.12b also includes the results previously presented in Figure 4.11b. The results for Turner et al. (1969) critical flow rate are also compared. The angle ( $\theta$ ) above the x-axis in figure (a) indicates the inclination of the well.....	59
Figure 4.13 – Simulated results shows the increase on wellbore liquid holdup over time using the proposed model with correlation for TPR proposed in this study. This increase in liquid content in the wellbore is often correlated in the field to liquid loading symptoms. ....	61
Figure 4.14 – Simulated results for decline in production rate over time using the correlation for the TPR proposed in this study, and Gray (1974) correlation. The sharp and sudden change gas rate indicates the liquid loading initiation. The explanation for the large divergence between the model proposed in this study and other popular flow correlation is a consequence of the difference in predicted bottomhole pressure for low gas rates as shown in Figure 4.10.....	62
Figure 4.15 – Schematic representation of the change in wellbore liquid holdup, for different times for the simulated case. ....	64



## **Abstract**

This thesis presents an improved model for gas-liquid two-phase flow in churn and annular flow regimes for small- and large-diameter in vertical and near-vertical pipes. This new model assumes that a net liquid film moves upward along the pipe wall and gas phase moves upward, occupying the majority of the central part of the pipes, and forming a gas core, in both flow regimes. The model is validated using field and laboratory experimental data from several different studies from the literature, in terms of pressure along the wellbore or bottomhole pressure for field conditions (for high-pressure flows in long pipes, and using hydrocarbons fluids), and pressure-gradient and liquid holdup for experimental laboratory data, for pipe diameters ranging from 0.0318 to 0.279 m (1.2520 to 11 in). The proposed model presents an overall better performance when compared to several other multiphase flow models widely used in the oil and gas industry.

This model is also tested in the application of prediction of liquid loading in gas wells. Liquid loading is generally associated with a reduction of ultimate recovery of gas wells. Liquid loading inception is simulated using nodal analysis technique. This study suggests that liquid loading initiates when the Inflow Performance Relationship (IPR) curve is tangent to the TPR curve. This study also proposes a new concept of a modified Tubing Performance Relationship (TPR) curve in order to predict the time liquid loading initiates and when the gas well stops flowing after reaching this condition. Field data is used for validation of this approach. The use of conventional models shows a significant mismatch predicting the inception of liquid loading, while the use of the tangent concept reduces this mismatch significantly.

## 1. Introduction<sup>1,2</sup>

Gas-liquid two-phase flow is widely existent in many industrial areas. In the chemical processing industry, two-phase flow is encountered easily in distillation towers and direct-contact heat exchangers. The nuclear power industry makes use of steam and water two-phase flows, where the fluid mixture works as a coolant to absorb heat from the reactor core. In the petroleum industry, gas-liquid two-phase flow occurs inside wellbores, risers, and pipelines, during production and transportation of hydrocarbons.

Hewitt (1982) described that among the four possible combinations of two-phase flows (gas-liquid, gas-solid, liquid-liquid, liquid-solid), gas-liquid two-phase flow is the most complex, as it includes the effects of gas compressibility and the deformable interface between the phases. For several decades, efforts have been focused on comprehending how the gas-liquid phases interact and flow inside pipes. Depending on the gas and liquid flow rates and fractions, pipe diameter and inclination, fluid properties, and conduit configurations, these two phases behave differently. The complication occurs due to the fact that the forces acting on the fluids such as buoyancy, inertia, viscosity, and surface tension vary as a function of phase distribution and conduit size and shape. The geometric configurations the flowing mixtures exhibit in the conduit are classified as flow regimes (this study uses the term “flow regime”, which is essentially the same as “flow patterns” as preferred by some other studies).

---

<sup>1</sup>This chapter previously appeared as E. Pagan, W. C. Williams, S. Kam, P. J. Waltrich, Modeling Vertical Flow in Churn and Annular Flow Regimes in Small- and Large-Diameter Pipes, Paper Presented and Published at BHR Group’s 10th North American Conference on Multiphase Technology 8-10th June 2016. It is reprinted by permission of Copyright © 2016 BHR Group. See Appendix for more details.

<sup>2</sup>Section 1.2 of this chapter previously appeared as Erika V. Pagan, Wesley Williams, and Paulo J. Waltrich, A Simplified Transient Model to Predict Liquid Loading in Gas Wells, Paper SPE-180403-MS presented at the SPE Western Regional Meeting held in Anchorage, Alaska, USA, 23-26 May 2016. It is reprinted by permission of Copyright 2016, Society of Petroleum Engineers Inc. Copyright 2016, SPE. Reproduced with permission of SPE. Further reproduction prohibited without permission. See Appendix for more details.

For vertical and near-vertical pipes, these flow regimes are commonly classified as bubble (bubbly or dispersed-bubble), slug, churn and annular flow regimes.

## **1.1 Flow Regimes**

The presence of two phases flowing through a pipe leads to the existence of flow regimes, which are characterized by the geometric distribution of the fluid phases in a pipe section. Many researches have tried to recognize and define these two-phase configurations using different methods, such as visualization through transparent pipes, photographic methods, X-radiography measurements, and multibeam gamma densitometry. The principle of each method and the problems in their application are summarized by Hewitt (1982). The photographic method using high speed camera is widely used, since it allows for flow visualization, and it is more reliable than only direct visual observation.

Diverse interpretations on visualization of flow behavior by different researchers have led to a lack of agreement in the description and classification of the flow regimes. The present study presents the generally encountered classification for flow regimes for gas-liquid flowing upward in a vertical and near-vertical pipe. Keeping a constant liquid flow rate in the pipe, and increasing the gas flow rate, the regimes change from bubble flow at low gas flow rate to slug flow, then to churn flow, and finally to annular flow at high gas rates. When flow configuration is in the annular flow regime, an increase in liquid rate leads to another flow regime called wispy annular flow. These regimes are represented by Figure 1.1, and are characterized as follows:

- Bubble (dispersed-bubble) Flow: The gas phase is present in form of dispersed bubbles uniformly distributed in the continuous liquid phase. This regime occurs when there are high liquid velocities and low gas velocities flowing through the tubing. Both phases move upwards. This regime can be further classified into bubbly or dispersed-bubble

flow. The former is represented by relatively fewer and larger bubbles moving faster than the liquid phase, while the latter is represented by several tiny bubbles transported by the liquid phase with same velocity (Brill and Mukherjee, 1999).

- Slug (Plug) Flow: Due the increase of gas content inside the pipe, bubbles get closer and coalesce, forming a series of bullet-shape bubbles called Taylor bubbles. These bubbles have their diameters close to the pipe diameter and they are axially symmetric. Taylor bubbles are separated from the pipe wall by a thin liquid film. The liquid film flows downwards while the Taylor bubbles move upwards. Liquid slugs moving upwards separate two consecutive Taylor bubbles. The liquid slugs contain small bubbles dispersed within them. The countercurrent liquid film creates these bubbles. The net liquid flow is upward.

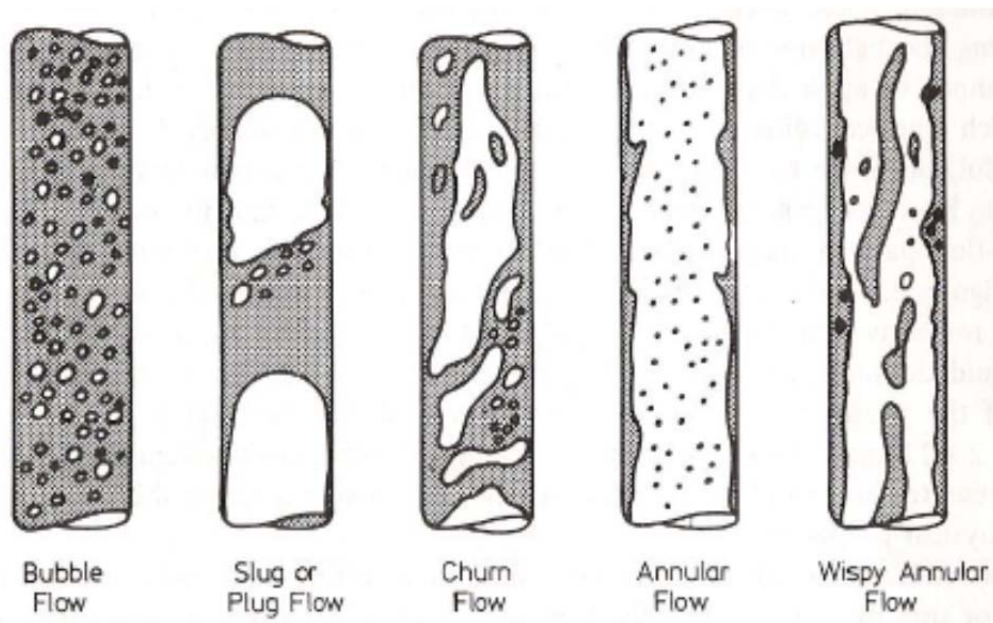


Figure 1.1 – Flow regimes for gas-liquid upwards flow in vertical pipes (Hewitt, 1982).

- Churn Flow: When the flow regime inside a pipe is in the slug flow condition and there is further increase in gas flow rate, the regime eventually changes to the churn regime. The

slugs are continuously destroyed by the high local concentration of gas phase, consequently the Taylor bubbles are distorted by the liquid phase. This regime is represented by a chaotic motion of the phases, since there is no clear boundary between the phases. More details about this flow regime are discussed later in this section.

- **Annular Flow:** This flow is characterized by a thin wavy layer of liquid near the pipe wall and a relatively fast gas core flowing through the center of the pipe. Entrained liquid droplets are generally present in the gas core and gas bubbles are generally entrained in the liquid film. More details about this flow regime is also presented later in this section.
- **Wispy Annular:** In this flow, droplets coalesce in the core creating large lumps or streaks, called wisps, due an increase of liquid rate.

In order to predict the pressure gradient in a wellbore, various multiphase flow models are used in the literature. They often use different sub-models or correlation coefficients for each flow regime because each regime has a unique hydrodynamic behavior. Thus, it is essential to develop accurate models for a wide range of flow regimes.

Waltrich (2012) stated that churn flow regime is generally encountered in producing gas wells under liquid loading conditions. However, Hewitt (2012) has described that churn flow regime is far less studied, thus less understood, than other flow regimes in vertical two-phase flows. The reason for the lack of mechanistic models to predict the hydrodynamic properties of churn flow is due to the highly chaotic and disordered nature of this flow regime (Kaya et al., 2001). According to Kaya et al. (2001), many times hydrodynamic models for slug flow regimes are used to model churn flow without any modifications. Other studies have suggested few modifications on previous validated slug flow models in order to develop a model to churn flow (Tengesdal et al., 1999).

## **1.2 Two-Phase Flow Modeling in Small and Large Diameter Pipes**

Although there are numerous studies to model the pressure gradient and liquid holdup in vertical pipes, most of them were originally developed for small pipe diameters (smaller than 0.1016 m (4 in)) (Poettmann and Carpenter, 1952; Hagedorn and Brown, 1965; Beggs and Brill, 1973; Gray, 1974). Some of the commercial multiphase flow simulators, widely used in the industry, have long and complex codes, most of which are tuned with field data and are not open to the public, and thus the understanding of the underlying assumptions and limitations behind such codes is limited.

Recent studies (Omebere-Yari and Azzopardi, 2007; Ali, 2009; Van der Meulen, 2012; Zabaras et al., 2013) have attempted to capture the behavior of two-phase flow in large-diameter vertical pipes ( $ID \geq 0.127$  m (5 in)). Some of these studies show experimentally that churn flow regime is commonly observed for a wide range of gas-liquid ratios for two-phase flows when the pipes have large diameters. It was also observed, more importantly, that the behavior of flow regimes is significantly different in large pipe diameters. For instance, slug flow regime is not experimentally observed in large pipe diameters, when it is expected to occur in small pipe diameters at the same flowing conditions (Omebere-Yari and Azzopardi, 2007; Ali, 2009; Van der Meulen, 2012; Zabaras et al., 2013).

The Bureau of Ocean Energy Management (2010) requires Worst Case Discharge (WCD) calculations prior to all wells being permitted in the Gulf of Mexico. During drilling activities, diameters larger than 0.254 m (10 in) are present in many portions of the well configuration. The use of multiphase flow models for large pipe diameters is essential to the calculation of WCD for offshore wells. The extension of existing mechanistic models and flow correlations, built based on small-diameter experiments, however, is still uncertain. SPE (2015)

raised the same concerns by stating that further research for correlations applicable at high flow rates in large pipe diameters is needed. Zabarar et al. (2013) also discussed the need of two-phase flow models for large diameter pipes for gas-lift applications within offshore risers.

Multiphase flow models are also suggested by some investigators to be used for the estimation of liquid loading initiation in gas wells (Skopich et al., 2015; Waltrich et al., 2015b). Liquid loading is generally defined as the inability of a producing gas well to lift the coproduced liquids up the tubing, resulting in liquid accumulation in the wellbore. One of the main problems associated with liquid loading is the sudden drop in gas production rates or “death” of the well. Decline curve analysis often fails to predict the sudden drop in gas production observed in the field (Lea et al., 2003), and this mismatch in production forecasting can have a significant impact on the prediction of ultimate recovery for gas wells. Thus, liquid loading can be associated with a reduction of ultimate recovery of gas wells. Therefore, it is clear to conclude that the development of a model to predict the production forecast for gas wells should include the liquid loading phenomenon and its transient effects.

Based on the need of more studies on churn flow regime and further development of two-phase flow models for large pipe diameters, this study proposes a model for gas-liquid two-phase flows that can be applied to churn and annular flow regimes in vertical and near-vertical pipes, for small and large pipe diameters. This study also proposes the use of this model to predict production forecast of gas wells, including the transient effects before and after liquid loading initiation, by use of the nodal analysis technique.

### **1.3 Objectives**

The objective of this thesis is to develop a model for gas-liquid two-phase flow in churn and annular flow regimes for small- and large-diameter in vertical and near-vertical pipes. This

model is intended to be used by the oil and gas industry for several different applications such as gas-lift operations, production of gas-condensate wells, Worst Case Discharge calculations, prediction of liquid loading initiation, and high-gas-volume fraction two-phase flows in general.

To accomplish this objective, the following tasks are carried out:

- Literature review of gas-liquid flow in vertical and near-vertical pipes for a broad range of pipe sizes.
- Collect experimental and field data available in the literature in terms of bottomhole pressure, pressure profile along the wellbore, pressure gradient and liquid holdup for vertical and near-vertical pipes, particularly for churn and annular flow regimes.
- Develop a model for churn and annular flow regimes, for vertical and near-vertical two-phase flows for tubes of small and larger diameters.
- Compare the model proposed in this study with the state-of-the-art models and commercial packages.
- Develop a model that can predict the transient behavior of liquid loading in gas wells.
- Describing the symptoms related to liquid loading often observed in the field using the model developed in this study.

## **1.4 Thesis Outline**

This thesis is divided into five chapters. Chapter 1 shows the problem and the motivation of this thesis, as well as the importance of this research and its objectives. The following chapters are divided in two main sections, the first section is related to the development of the multiphase flow model for churn and annular flow, and the second section is related to the application of this model to the prediction of liquid loading initiation. Chapter 2 reviews the basic theory on two-phase flow in vertical and near-vertical pipes, as well as, details the concepts of churn and



annular flows. In addition, it discusses the current methods and their limitations in prediction of liquid loading in gas wells. Chapter 3 describes how the model for churn and annular flow for vertical and near-vertical pipes was developed. It also presents the concept this study suggests to be applied to predict the inception of liquid loading in gas wells. Chapter 4 presents the results of the comparison of the churn and annular model simulations on the prediction of pressure gradient and liquid holdup using several different experimental data, and on the prediction of bottomhole pressure, and pressure along the wellbore using field data. It also presents the simulations using different models and correlations available in the literature. These simulations were performed using PIPESIM software (PIPESIM, 2013). In addition to this, Chapter 4 presents the results of the prediction of liquid loading initiation using the concept proposed in this study. Finally, chapter 5 summarizes the content of this study as well as presents the conclusions obtained from this investigation, and suggests recommendations for future work.

## 2. Literature Review <sup>1,2</sup>

This chapter is subdivided into two main sections. The first section outlines the fundamentals of two-phase flow. The second section presents a literature review based on the current models used in the prediction of liquid loading initiation.

### 2.1 Two-Phase Flow Modeling

For a clear understanding of the content of this thesis, the fundamentals of two-phase flow is briefly presented. In the next sections, the concepts of liquid holdup, void fraction, pressure gradient, superficial velocities, and flow regimes are explained.

#### 2.1.1 Liquid Holdup

Void fraction ( $\alpha$ ) is defined as volumetric fraction of gas phase contained in a section of a pipe. Void fraction is commonly defined by the following expression,

$$\alpha = \frac{V_g}{V} \quad (2.1)$$

where  $V_g$  is the volume of gas present in a certain pipe segment, and  $V$  is the total volume of the pipe segment.

The liquid holdup is the complement of void fraction (or liquid fraction in the considered pipe segment), which is represented by the following expression,

$$H_L = (1 - \alpha) = \frac{V_l}{V} \quad (2.2)$$

---

<sup>1</sup>Section 2.1 of this chapter previously appeared as E. Pagan, W. C. Williams, S. Kam, P. J. Waltrich, Modeling Vertical Flow in Churn and Annular Flow Regimes in Small- and Large-Diameter Pipes, Paper Presented and Published at BHR Group's 10th North American Conference on Multiphase Technology 8-10th June 2016. It is reprinted by permission of Copyright © 2016 BHR Group. See Appendix for more details.

<sup>2</sup>Section 2.2 of this chapter previously appeared as Erika V. Pagan, Wesley Williams, and Paulo J. Waltrich, A Simplified Transient Model to Predict Liquid Loading in Gas Wells, Paper SPE-180403-MS presented at the SPE Western Regional Meeting held in Anchorage, Alaska, USA, 23-26 May 2016. It is reprinted by permission of Copyright 2016, Society of Petroleum Engineers Inc. Copyright 2016, SPE. Reproduced with permission of SPE. Further reproduction prohibited without permission. See Appendix for more details.

The prediction of liquid holdup in a pipe segment is one of the most important parameters in the determination of the pressure gradient for two-phase flow in pipes.

### 2.1.2 Pressure Gradient

Pressure gradient is defined as the pressure drop per unit length of pipe. It is represented by the term  $-dp/dl$ , where  $dp$  is the pressure drop and  $dl$  is the unit length of the pipe. The negative sign is usually used in front of the term to turn the term positive, since the pressure generally drops for upward flow in pipes (Shoham, 2006).

The total pressure gradient is commonly represented by the sum of three components: pressure gradient due to friction, pressure gradient due to gravitation effects, and pressure gradient due to flow acceleration. The total pressure gradient can be represented by the following equation,

$$-\left(\frac{dp}{dl}\right) = -\left[\left(\frac{dp}{dl}\right)_f + \left(\frac{dp}{dl}\right)_g + \left(\frac{dp}{dl}\right)_{acc}\right] \quad (2.3)$$

where  $-dp/dl$  is the total pressure gradient,  $-(dp/dl)_f$  is the frictional component,  $-(dp/dl)_g$  is the gravitational component,  $-(dp/dl)_{acc}$  is the accelerational component.

The pressure gradient equation for steady-state flow in pipes uses the principles of mass and momentum conservation. For two-phase flow, the frictional component results from the pressure drop due to friction losses at the pipe wall, as well as the friction due to the shear stress between the phases. The gravitational component accounts for the elevation change of the fluids in the gravitational field. The accelerational component is a consequence of the changes in velocities along the pipe length. For adiabatic flows and low flow velocities, this last term is usually very small in comparison to the first two terms, and consequently, is often neglected (Brill and Mukherjee, 1999). In this study, the accelerational component is also neglected.

Figure 2.1 shows a graphical representation of the pressure gradient as a function of gas flow rate, for a constant liquid rate. For low gas rates, the gravitational component of the pressure gradient is dominant, because the fraction of liquid inside the pipe (liquid holdup) is high. As the gas rate increases, liquid holdup decreases and the gravitational component also decreases. At the same time, the frictional component increases for larger gas rates. The sum of the gravitational and the frictional components provides the total pressure gradient, which is represented by the bold line in Figure 2.1.

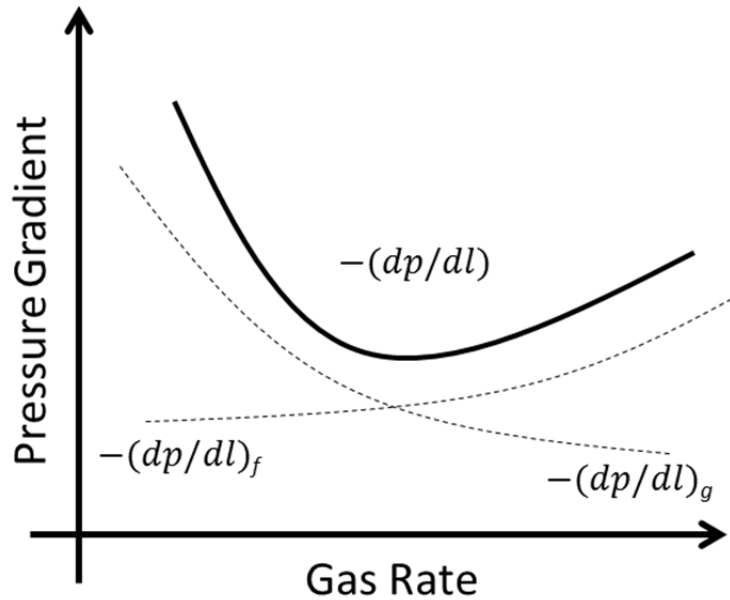


Figure 2.1 – Graphical representation of the total pressure gradient for gas-liquid flow in vertical- or near-vertical pipes (Modified after Shoham, 2006).

The pressure gradient representation in Figure 2.1 can also be viewed as a Tubing Performance Relationship (TPR) curve, which is represented by the wellbore bottomhole flowing pressure as a function of the gas rate, if a fixed wellhead pressure and a constant pressure gradient throughout the wellbore are assumed,

$$p_{wf} = \frac{dp}{dl} MD + p_{wh} \quad (2.4)$$

where  $p_{wf}$  is the wellbore flowing bottomhole pressure,  $MD$  is the wellbore measured depth, and  $p_{wh}$  is the wellhead pressure.

The shape of the TPR curve depends on the gas and liquid rates, as well as on the individual components in the production system (i.e., completions configuration, wellbore and flowline length and diameter, choke valves, among others). These components are responsible for the flow pressure changes from the reservoir to the surface. The liquid and gas volumetric flow rate can be represented in terms of superficial velocities. The definition of superficial velocity is described next.

### 2.1.2.1 Superficial Velocities

The superficial velocity of the liquid phase ( $u_{sl}$ ) or the gas phase ( $u_{sg}$ ) is the ratio of the volumetric flow rate of the phase ( $q_l$  for the liquid phase or  $q_g$  for the gas phase) divided by the total cross sectional area of the pipe ( $A$ ). The liquid superficial velocity is defined as,

$$u_{sl} = \frac{q_l}{A} \quad (2.5)$$

and the gas superficial velocity as,

$$u_{sg} = \frac{q_g}{A} \quad (2.6)$$

The superficial velocity characterizes the velocity that would have happened if only one phase is flowing in a pipe segment. A dimensionless form of the superficial velocities for liquid and gas are represented by the Froude number, defined by the following equations (Hewitt and Wallis, 1963):

$$u_{sl}^* = u_{sl} \left[ \frac{\rho_l}{gd(\rho_l - \rho_g)} \right]^{0.5} \quad (2.7)$$

$$u_{sg}^* = u_{sg} \left[ \frac{\rho_g}{gd(\rho_l - \rho_g)} \right]^{0.5} \quad (2.8)$$

where  $\rho_g$  is the gas-phase density,  $\rho_l$  is the liquid-phase density,  $g$  is the gravitational constant, and  $d$  is the diameter of the pipe.

The model proposed in this study applies the mass and momentum conservation equations for churn and annular flows. Therefore, before applying the conservation equations, it is important to characterize the main features of each flow regime. The next two sections describe the main details and the differences for churn and annular flows.

### 2.1.3 Annular Flow

Annular flow in vertical and near-vertical two-phase flow is characterized by a high-speed gas core containing entrained liquid droplets, as shown in Figure 2.2a. This flow regime features a thin liquid film around the pipe wall that may contain entrained gas bubbles. In vertical and near-vertical annular flow, the liquid film is thin and relatively uniform around the pipe perimeter. Waves are formed on the liquid film by the drag of the high-velocity gas core. These waves are the source of the entrained droplets in the gas core when the shear from the gas core against the liquid film breaks off the tip of the waves. The entrained droplets occasionally are re-deposited in the liquid film downstream where they were originally formed, as they move randomly in the gas core and are carried up by the gas stream (Hewitt and Hall-Taylor, 1970).

### 2.1.4 Churn Flow

Churn flow regime is a very chaotic flow. Some investigators have affirmed that the physics of this regime is very difficult to be modeled and described experimentally due to the complexity of this flow regime (Ansari et al., 1994; Shoham, 2006). According to Barbosa et al. (2001), churn flow regime is similar to annular flow regime in that a liquid film is present on the

pipe wall and a large gas core is positioned in the middle of the pipe. However, in the churn flow regime, the liquid film flows in an oscillatory manner, upwards and downwards because the gas velocity is not high enough to carry the liquid continuously upward.

Large waves are typically created on the liquid film, due to the drag force exerted by the gas phase flowing upwards at a velocity higher than the net-upward liquid film velocity. The large waves frequently break up and a large fraction of the liquid can be entrained as droplets or lumps of liquid. Upstream to the large liquid film waves, a thin liquid film flows downwards, and part of this film is carried upwards by subsequent large waves flowing upwards. Hewitt et al. (1985) also experimentally visualized such a characteristic. Churn flow phase distribution is represented by the schematic representation in Figure 2.2b.

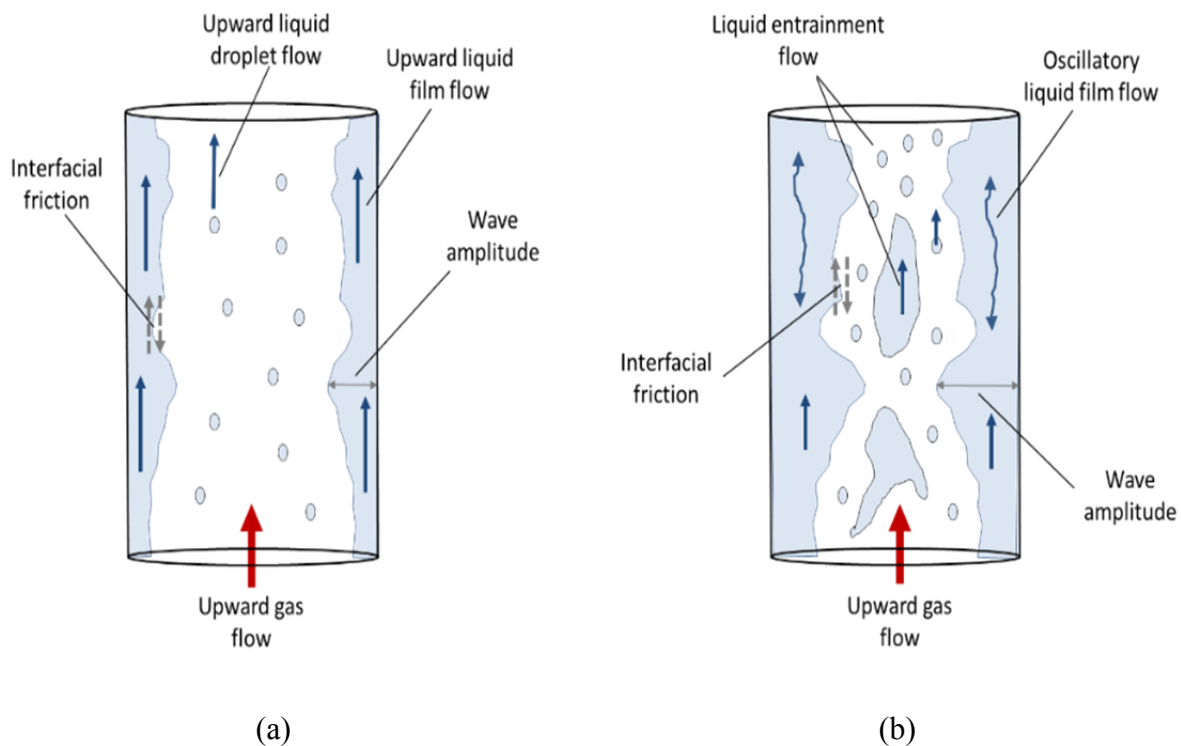


Figure 2.2 - A schematic representation of distribution of phases and mass transfer mechanisms for (a) annular flow and (b) churn flow. These representations are based on experimental observations of Waltrich et al. (2013), using a clear vertical pipe (42 m long, and 0.048 m internal pipe diameter).

The churn flow regime has been known to occur between the slug and the annular flow regimes, although a direct transition from slug or even from bubbly flow directly to annular flow may happen at very high liquid flow rates (Jayanti and Hewitt, 1992). Some researchers do not recognize churn flow as a separate flow regime because of its similarity with annular flow. Many other researchers believe that this configuration is simply a transition regime. For instance, Taitel et al. (1980) and Dukler and Taitel (1986) describe churn flow regime as an entrance phenomenon preceding a downstream stable slug flow for a pipe of enough length. Waltrich et al. (2013), however, recently stated that the churn flow regime exists and should be admitted as a separate regime. Their conclusion was based on experimental observations, through video recordings and liquid holdup measurements by using a 42 m long, 0.048 m internal diameter, vertical tube system.

### **2.1.5 Correlations Available in the Literature**

There are several correlations available in the literature developed to model the hydrodynamics of two-phase flows in wellbores under different flow regimes. Some of these correlations are well accepted by the oil and gas industry and widely used to estimate pressure gradient in wellbores.

In this study, some of these correlations are used to simulate the data collected in order to compare the performance of the model proposed in this study in relation to other correlations currently available in software packages.

The correlations selected for the comparison in this study (Duns and Ros, 1963; Gray, 1974; Ansari et al., 1994; OLGA, 2000) are included in PIPESIM software (PIPESIM, 2013). This section carries out a brief literature review on these correlations, based on the conditions of which each flow correlation used in this study was developed and validated.



### **2.1.5.1 Duns and Ros (1963) Correlation**

Duns and Ros (1963) developed their empirical correlations based in three different regions determined by them according to the gas rate. Region I is a region of low gas rates, which is composed by a continuous liquid phase comprising bubble flow, plug flow (similar to slug flow – more stable bullet-shaped gas plugs in the continuous liquid phase) and part of the froth-flow (also called churn) regime. Region II is a region of intermediate gas rates, which the continuous phase alternate between liquid and gas phases. Region II comprises slug flow and the remainder of the froth-flow regime. Region III is a region of high gas rate, which is composed by a continuous gas phase comprising mist-flow regime.

Duns and Ros (1963) stated that their correlation can be applied over an extensive range of field operating conditions. Their correlation was validated using approximately 20,000 data points from about 4,000 gas-liquid two-phase flow tests (Li, 2013). Besides water, other fluids with different densities, surface tension and viscosity were also used in their experiments as lubricating oil, gas oil and mineral spirit (Li, 2013). The data were measured in a vertical pipe section of 10 m (32.8 ft) height and nominal internal diameters of 0.032, 0.0802, and 0.1423 cm (1.2598, 3.1575, and 5.6024 in) (Takacs, 2001). Superficial liquid velocities ranged from 0 to 100 m/s, and superficial gas velocities from 0 to 32 m/s (Li, 2013). Water cut ranged from 0 to 100 % (Takacs, 2001).

### **2.1.5.2 Gray (1974) Correlation**

The Gray (1974) empirical correlation was developed for vertical gas wells with coproducing liquids. Flow is treated as single-phase. Thus, no flow regime is considered. They used 108 test data from wells, in which 88 of these were reported to coproduce some liquid (Li, 2013). Their results for prediction of pressure gradient were superior to the predictions using

conventional dry gas models. However, the accuracy of the Gray (1974) method is still uncertain for some conditions (Li, 2013): for mixture velocity (sum of superficial liquid velocity and superficial liquid velocity) greater than 15.24 m/s (50 ft/s), for nominal pipe diameters greater than 0.0889 m (3.5 in), liquid condensate and gas ratio greater than  $2.81 \times 10^4 \text{ m}^3/\text{sm}^3$  (50 bbl/MMscf), and water and gas ratio greater than  $2.81 \times 10^5 \text{ m}^3/\text{sm}^3$  (5 bbl/MMscf).

#### **2.1.5.3 Ansari et al. (1994) Correlation**

The Ansari (1994) mechanistic model is composed of a set of independent correlations to predict pressure drop and liquid holdup in bubble, slug, and annular flow regimes, as well as by a model to predict the transition between these flow regimes. Churn flow was not considered. Their method was validated using Tulsa Fluid Flow Project (TUFFP) well data bank containing 1,712 well cases with a wide range of conditions as nominal diameter varying from 0.0254 to 0.2032 m (1 to 8 in), oil rates from 0 to 4,300  $\text{sm}^3/\text{d}$  (0 to 27,000 stb/d), gas rates from 0.46 to 33,500  $\text{Msm}^3/\text{d}$  (1.5 to 110,000 Mscf/d), and oil gravity from 9.5 to 112 °API.

#### **2.1.5.4 OLGA (2000) Correlation**

The OLGA (2000) mechanistic model was developed for predictions of steady-state pressure drop, liquid holdup, and flow regime transitions (Bendiksen et al., 1991). OLGA (2000) model was validated using SINTEF Two-Phase Flow Laboratory (near Trondheim, Norway) data, as well as other data from literature and field. SINTEF experimental loop was designed to operate at conditions close to field conditions. The loop is 800 m long with 0.0254 m (8 in) internal diameter. Naphtha, diesel oil, or lube oil was used as liquid phase. Nitrogen was used as gas phase. Pressures ranged from 20 to 95 barg (Rygg and Gilhuus, 1990). Superficial liquid velocities up to 4 m/s and superficial gas velocities up to 13 m/s were tested (PIPESIM, 2013). The model uses three separate mass continuity equations for gas, liquid bulk, and liquid droplets.

In addition, one momentum balance equation for gas and liquid droplets, and other for the liquid film. One energy conservation equation is also included in the model (Bendiksen et al., 1991). Their determination of flow regime is based in two groups: distributed flow and separated flow. The former includes bubble and slug flow regimes, and the latter includes what they call stratified and annular mist flow regimes.

## 2.2 Liquid Loading

This section discusses the current methods and their limitations on prediction of the inception of liquid loading in gas wells. Liquid loading is a phenomenon that happens to all gas wells, which co-produce some liquids, at some stage of their production life cycle (Lea et al., 2003). This phenomenon is generally associated with a reduction of ultimate recovery of gas wells. In order to accurately forecast gas wells production, prediction of liquid loading initiation is necessary.

### 2.2.1 Turner et al. (1969) Droplet Model

Models commonly used to predict the initiation of liquid loading utilize the idea of critical gas velocity to determine when liquid loading starts. The most widely accepted method to predict liquid loading initiation is the droplet transport model of Turner et al. (1969). In their approach, the balance between downward gravitational force and upward gas drag force on a liquid droplet is solved to determine the minimum velocity ( $u_{min}$ ) to lift the largest droplet flowing with the gas stream, given by the following expression,

$$u_{min} = 5.46 \left[ \frac{\rho_l - \rho_g}{\rho_g^2} \sigma \right]^{1/4} \quad (2.9)$$

where  $\sigma$  is the surface tension (in N/m),  $\rho_g$  is the gas density (in kg/m<sup>3</sup>) and  $\rho_l$  is the liquid density (in kg/m<sup>3</sup>).

The development of Equation (2.9) by Turner et al. (1969) was based on a comparison between their droplet model and a liquid film transport model. Both models were compared to field data, and the droplet model showed a superior performance in predicting liquid loading. However, the field data collected by Turner et al. (1969) only included surface measurements, and key variables such as surface tension and fluid densities were simply estimated based on generic fluid property correlations. Another important information missing in their work was the fact that the work of Turner et al. (1969) did not clearly define how they classified wells as “loaded” or “unloaded”. Furthermore, Westende et al. (2007) and Waltrich et al. (2105a) have shown experimentally that even for gas velocities lower than the minimum critical velocity of Turner, given by Equation (2.9), liquid droplets flow upwards and not downwards as suggested by Turner et al. (1969). Another limitation of the model proposed by Turner et al. (1969) is the fact that Equation (2.9) only calculates the minimum flow rate for liquid loading initiation. This method cannot be used to simulate the transient effects of liquid loading in gas wells, i.e., the time the well starts suffering from liquid loading, and when the gas well stops production after liquid loading initiation.

### **2.2.2 Minimum Pressure Point and Nodal Analysis**

Another commonly used method to predict liquid loading initiation includes the concept of the minimum pressure point in the wellbore curve, as shown in Figure 2.3 (Lea et al., 2003). This concept assumes that when the reservoir Inflow Performance Relationship (IPR) curve intersects the Tubing Performance Relationship (TPR) curve to the left or at the minimum pressure point, liquid loading is initiated. This method is often correlated to the transition between annular to churn (or intermittent) flow regime based on the minimum pressure of the TPR curve, which is also used as criterion for liquid loading initiation in some studies (Skopich

et al., 2015; Riza et al., 2015). In Figure 2.3, the difference between  $IPR_1$  and  $IPR_2$  is the average reservoir pressure, where it is known that the reservoir pressure naturally depleats as consequence of the gas production.

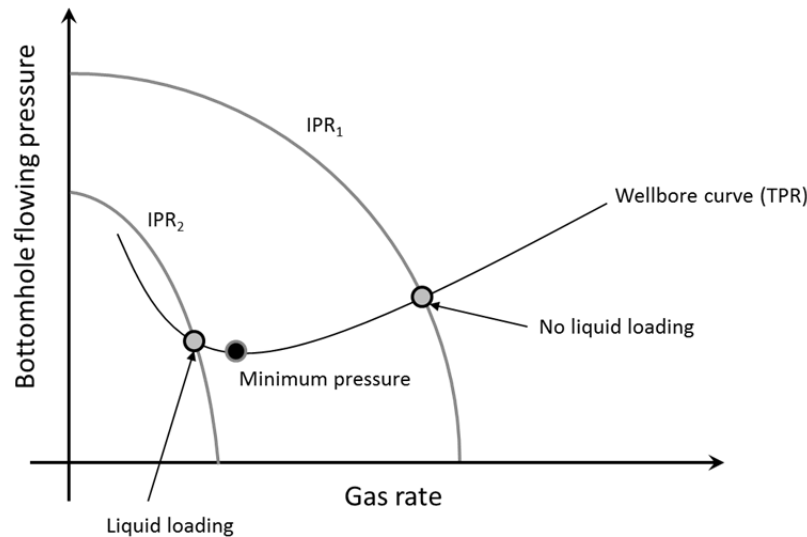


Figure 2.3 – The nodal analysis technique used to predict liquid loading in gas wells. The intersection between the IPR and TPR curves to left of the minimum pressure point defines if the well is under liquid loading conditions (Lea et al., 2003).

A limitation for this method is that it cannot explain the production from reservoirs with low permeability, which normally present IPR curves that intercepts the TPR curve to the left of the point of minimum pressure, and these wells can still flow without suffering from liquid loading symptoms (Lea et al., 2003). Thus, the concept of minimum pressure may not be the most appropriate to predict liquid loading initiation since it may work for some reservoirs, but not for others, depending, for instance, on the reservoir permeability.

### 2.2.3 Coupled Reservoir/Wellbore Modeling

Recently, some investigators (Zhang et al., 2009; Yusuf et al., 2010; Hu et al., 2010) have proposed coupled reservoir/wellbore modeling to predict liquid loading in transient conditions.

Although these models provide reasonable solutions for liquid loading in transient conditions, some of these models include the use of commercial simulators or sophisticated modeling techniques that cannot be easily implemented using simple reservoir and tubing performance relationships. This study believes that one of the main reasons for the wide acceptance of the droplet model of Turner is due to the fact that Equation (2.9) gives a very simple relationship to indicate liquid loading initiation, which can be easily understood by most engineers. Therefore, it is important to develop a simplified model to predict liquid loading under transient conditions.

Other investigators have already proposed simplified methods to describe liquid loading under transient conditions using simple reservoir and tubing performance relationships. For instance, Oudeman (1990) proposed the use of multiphase reservoir performance and vertical flow performance of the tubing to improve prediction of wet-gas-well performance and liquid loading. To the knowledge of the authors, Oudeman's work was one of the first attempts to couple the reservoir performance to the tubing flow performance in order to explain liquid loading in gas wells under transient conditions. Following his approach, Douisi et al. (2006) has proposed the use of reservoir inflow performance coupled with a tubing flow performance curve to explain a process of water buildup and drainage in gas wells under transient liquid loading conditions. Douisi et al. (2006) also defined a condition called "metastable flow" as subcritical rates that a gas well would flow under liquid loading conditions.

Some authors (Chupin et al., 2007; Veeken et al., 2010; Whitson et al., 2012) have also shown the observation of metastable flow using field data. More recently, Limpasurat et al. (2015) have proposed the use of a new boundary condition for a coupled reservoir/wellbore modeling method that was validated with field data. These authors concluded that this new

boundary condition improves the prediction of transient effects for gas wells under liquid loading and also enhances the model previously proposed by Dousi et al. (2006). They also concluded that this new boundary condition can show the metastable flow observed in the field, as originally suggested by Dousi et al. (2006). However, Dousi et al. (2006) and Limpasurat et al. (2015) still have to use the minimum velocity criterion of Turner et al. (1969) to trigger liquid loading conditions.

Although the recent attempts of coupled reservoir/wellbore modeling have shown improvements on the understanding of liquid loading, simplified transient models are still exceptions rather than the norm. With the exception of the models using proprietary codes (which do not fully disclose all assumptions and details about their approach), all the other models discussed in this study use the minimum velocity criterion of Turner et al. (1969) to trigger liquid loading, even though the accuracy of Turner's droplet model has been recently questioned by many authors (Oudeman, 1990; Westende et al., 2007; Veeken et al., 2010; Skopich et al., 2015). Thus, a simplified model might encourage engineers to replace the use of the widely accepted model of Turner for more accurate methods that are as simple as Turner's approach.

### 3. Models Description <sup>1,2</sup>

This chapter is divided into two main sections. The first section describes the model proposed in this study for churn and annular flow. The second main section presents the concept for liquid loading inception prediction proposed in this study.

#### 3.1 Churn and Annular Flow Modeling

This study proposes a model for churn and annular flows in small and large diameters, in vertical and near-vertical pipes. This model is based on an approach originally proposed by Jayanti and Brauner (1994) for the churn flow regime in vertical pipes validated for small diameters.

##### 3.1.1 Momentum Equations

Figure 3.1 shows the force balance concept applied to churn and annular flows in this study. The inner control volume (Figure 3.1a) is used for the gas core, and the outer control volume (Figure 3.1b) is used for the entire gas and liquid phase in the cross-sectional area of the pipe. The liquid entrainment, in the gas core, for both churn and annular flow regimes, is assumed to be part of the liquid film, and the gas entrainment in the liquid film is neglected. In experimental observations (Hewitt et al., 1985), only few gas bubbles are observed in the liquid film.

Figure 3.1a illustrates the forces acting on the gas core segment with the cross-sectional area  $A_c$  and length  $dl$ .

---

<sup>1</sup>Section 3.1 of this chapter previously appeared as E. Pagan, W. C. Williams, S. Kam, P. J. Waltrich, Modeling Vertical Flow in Churn and Annular Flow Regimes in Small- and Large-Diameter Pipes, Paper Presented and Published at BHR Group's 10th North American Conference on Multiphase Technology 8-10th June 2016. It is reprinted by permission of Copyright © 2016 BHR Group. See Appendix for more details.

<sup>2</sup>Section 3.2 of this chapter previously appeared as Erika V. Pagan, Wesley Williams, and Paulo J. Waltrich, A Simplified Transient Model to Predict Liquid Loading in Gas Wells, Paper SPE-180403-MS presented at the SPE Western Regional Meeting held in Anchorage, Alaska, USA, 23-26 May 2016. It is reprinted by permission of Copyright 2016, Society of Petroleum Engineers Inc. Copyright 2016, SPE. Reproduced with permission of SPE. Further reproduction prohibited without permission. See Appendix for more details.



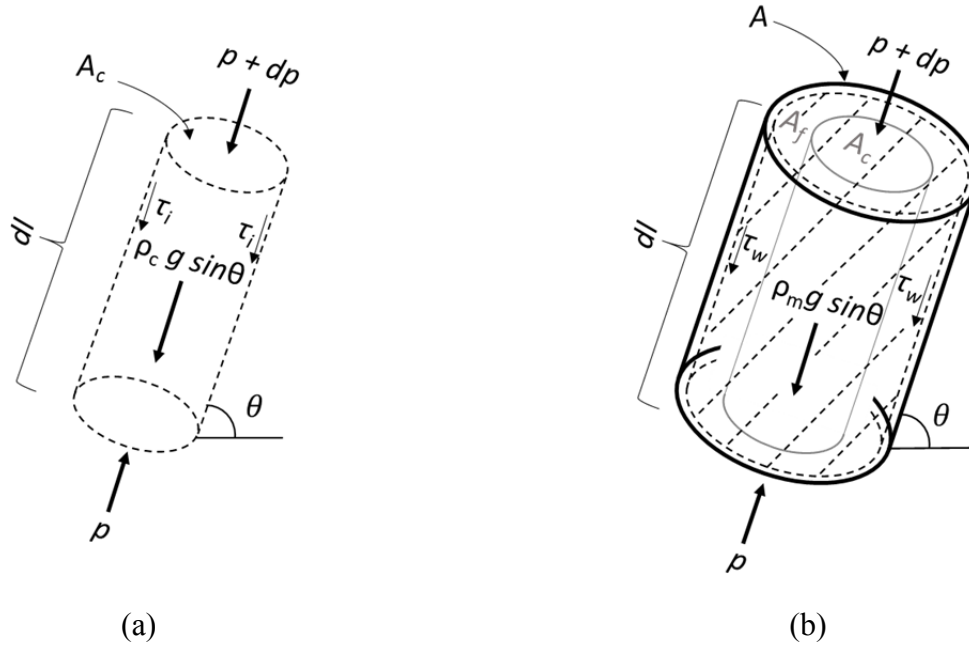


Figure 3.1 - Force balance for a pipe segment for churn and annular flow regimes on (a) gas core and (b) total cross-sectional area (including liquid film and gas core).

The net flow rates of both gas and liquid phases are upward, and the gas phase moves faster than the liquid phase. Thus, shear stress at the interface between the gas and liquid phases,  $\tau_i$ , is introduced to consider the interaction between the phases. Figure 3.1b illustrates the forces acting on the total cross-sectional area of the pipe  $A$ , which is the sum of the cross-sectional areas of the gas core,  $A_c$ , and liquid film,  $A_f$ . The interaction between the liquid film and the wall is considered by the shear stress,  $\tau_w$ .

The momentum (force) balance equations to the inner and outer control volumes are given, respectively by (if the acceleration term is negligible) (Jayanti and Brauner, 1994),

$$-\frac{dp}{dl} = \frac{4\tau_i}{d\sqrt{\alpha}} + \rho_g g \sin\theta \quad (3.1)$$

$$-\frac{dp}{dl} = \frac{4\tau_w}{d} + [\rho_g \alpha + \rho_l (1 - \alpha)] g \sin\theta \quad (3.2)$$

where  $dp/dl$  is the pressure gradient for the pipe segment,  $d$  is the diameter of the pipe,  $\theta$  is the inclination angle (i.e.,  $\theta = 90^\circ$ , if vertical),  $\alpha$  is the void fraction,  $\rho_g$  and  $\rho_l$  are the gas and

liquid densities,  $\tau_i$  is the interfacial shear stress,  $\tau_w$  is the wall shear stress, and  $g$  is the gravitational acceleration.

The two momentum balance Equations (3.1) and (3.2) are solved for the pressure gradient and void fraction. The solution of these two equations requires the calculations of the interfacial shear stress ( $\tau_i$ ) and the wall shear stress ( $\tau_w$ ). The procedure to calculate  $\tau_i$  and  $\tau_w$  is presented in the next section.

A caution must be taken during the application of this model for pipes with large inclination angles, because churn flow is gradually suppressed with increasing inclination angle, completely disappearing at an angle of between 20 and 30 degrees from vertical direction (Jayanti and Brauner, 1994). Therefore, the model proposed here is intended to provide reasonable results for inclination angles up to 15 degrees (i.e.,  $75^\circ \leq \theta \leq 90^\circ$ ).

### 3.1.2 Wall and Interfacial Shear Stress

In the churn flow regime, the liquid motion is oscillatory. However, the net liquid rate is upward. Thus, Jayanti and Brauner (1994) proposed that the average wall shear stress should be calculated based on the net liquid flow rate, neglecting the variation with time. As in the annular flow regime, the net liquid film flows always upward along the pipe wall. Thus, the wall shear stress,  $\tau_w$ , is calculated from the following relationship for both annular and churn flow regimes,

$$\tau_w = \frac{1}{2} \rho_l f_l \left( \frac{u_{sl}}{1 - \alpha} \right)^2 \quad (3.3)$$

where  $u_{sl}$  is the superficial liquid velocity, and  $f_l$  is the friction factor within the liquid film. This equation represents wall shear stress for single-phase flow, considering only the liquid phase is in contact to the pipe wall. For Reynolds number on the liquid film ( $Re_{lf}$ ) smaller than 2,100 (laminar flow), the Fanning friction factor for laminar flow is used,

$$f_l = \frac{16}{Re_{lf}} \quad (3.4)$$

and for  $Re_{lf}$  greater than 2,100 (turbulent flow), Blasius equation for smooth pipes is used,

$$f_l = \frac{0.079}{Re_{lf}^{0.25}} \quad (3.5)$$

where,

$$Re_{lf} = \frac{u_{lf} \rho_l d}{\mu_l} \quad (3.6)$$

where  $\mu_l$  is the liquid-phase viscosity.  $Re_{lf}$  includes the actual liquid film velocity within the film ( $u_{lf}$ ), which is given by,

$$u_{lf} = \frac{u_{sl}}{1 - \alpha} \quad (3.7)$$

The interfacial shear stress between the gas core and the liquid film is calculated using Equation (3.8), which is analogous to Equation (3.3),

$$\tau_i = \frac{1}{2} \rho_g f_i \left( \frac{u_{sg}}{\alpha} \right)^2 \quad (3.8)$$

where  $u_{sg}$  is the superficial gas velocity. Equation (3.8) can be used since the gas velocity is generally much larger than the liquid velocity when the fluids are flowing under churn or annular flow regimes. Thus, the liquid velocity is neglected, and the interfacial shear stress is calculated based on single-phase gas flow.

Based on an analysis from the experimental results of Govan et al. (1991), Jayanti and Brauner (1994), which developed their model for churn flow only, suggest that the interfacial friction factor ( $f_i$ ) should be calculated by the average of two previously published correlations, represented by  $f_{i,B}$  and  $f_{i,W}$  as follow,

$$f_i = \frac{1}{2}(f_{i,W} + f_{i,B}) \quad (3.9)$$

where  $f_{i,W}$  was originally an empirical correlation proposed by Wallis (1969) assuming thin liquid films in pipes and  $f_{i,B}$  was originally an empirical correlation proposed by Bharathan et al. (1978). The present study uses the same average presented in Equation (3.9) for calculation of interfacial friction factor ( $f_i$ ) for both churn and annular flow regimes. However, for  $f_{i,B}$  the correlation of Bharathan and Wallis (1983) is used instead, as suggested by Alves (1994). This correlation provides best results for churn and annular flow regimes, and it is given by,

$$f_{i,B} = 0.005 + 10^{(-0.56 + \frac{9.07}{d^*})} \left[ \frac{d^*(1 - \alpha)}{4} \right]^{(1.63 + \frac{4.74}{d^*})} \quad (3.10)$$

where

$$d^* = d \sqrt{\frac{(\rho_l - \rho_g)g}{\sigma}} \quad (3.11)$$

and  $\sigma$  is the surface tension between gas and liquid. Furthermore, this study proposes the use of the general equation for interfacial friction factor proposed by Wallis (1969) for  $f_{i,W}$  as given by,

$$f_{i,W} = 0.005 \left( 1 + 300 \frac{\delta}{D} \right) \quad (3.12)$$

where  $\delta/D$  is the dimensionless liquid film thickness in the pipe. This last term can easily be represented in terms of void fraction ( $\alpha$ ) since void fraction can be interpreted by the cross-sectional area of the gas core,  $A_c$ , divided by the cross-sectional area of the pipe  $A$ . Thus, this study proposes Wallis (1969) modified interfacial friction factor without assumption of thin liquid film in pipes for churn flow regime, given by,

$$f_{i,W} = 0.005 + 0.75 (1 - \sqrt{\alpha}) \quad (3.13)$$

and Wallis (1969) modified interfacial friction factor equation with assumption of thin liquid film in pipes for annular flow regime, given by,

$$f_{i,w} = 0.005 + 0.375 (1 - \alpha) \quad (3.14)$$

### 3.1.3 The Churn to Annular Flow Transition

The transition from churn to annular flow in this study uses two different criteria depending on the pipe size. For pipe diameters equal to and smaller than 0.0508 m (2 in), the flow reversal criterion (assumption that all liquid film that was flowing in both upward and downward directions starts to flow only upwards) proposed by Wallis (1969) is used. This commonly used criterion can be easily observed experimentally and offers simple relationships to determine the transition from churn to annular flow regimes (Hewitt and Wallis, 1963; Pushkina and Sorokin, 1969; Taitel et al., 1980). This criterion states that this transition occurs when the dimensionless superficial gas velocity  $u_{sg}^*$  equals to the unit (Waltrich et al., 2013), i.e.,

$$u_{sg}^* = u_{sg} \left[ \frac{\rho_g}{gd(\rho_l - \rho_g)} \right]^{0.5} = 1 \quad (3.15)$$

For pipe diameters larger than 0.0508 m (2 in), the condition for flow reversal is used as suggested by Pushkina and Sorokin (1969), which is written in terms of Kutateladze number ( $K_{ug}$ ),

$$K_{ug} = u_{sg} \rho_g^{0.5} [g\sigma(\rho_l - \rho_g)]^{-0.25} \quad (3.16)$$

where the annular flow occurs when  $K_{ug} \geq 3.2$ , and the churn flow occurs when  $K_{ug}$  is  $< 3.2$ .

### 3.1.4 The Slug/Bubble to Churn Flow Transition

In this study, the transition from slug to churn, or bubble to churn flow, is also based on two different criteria, depending on the pipe size. The pipe diameter criteria used here follows

the work of (Zabaras et al., 2013), which suggests that Taylor bubbles cannot be sustained in vertical two-phase flows for pipe diameters larger than,

$$d_T = 30 \sqrt{\frac{\sigma}{g(\rho_l - \rho_g)}} \quad (3.17)$$

For diameters smaller or equal to  $d_T$ , the model of Brauner and Barnea (1986) is used for the slug-to-churn flow transition. According to their study, the transition occurs when the liquid holdup in the liquid slug ( $h_{sl}$ ) falls below a minimum value of 0.48 due to increase in gas rate. According to these authors, the excessive aeration causes the collapse of the liquid slug and the transition to churn flow regime. The liquid holdup in the liquid slug is correlated by,

$$h_{sl} = 1 - 0.058 \left\{ 2 \left[ \frac{0.4\sigma}{g(\rho_l - \rho_g)} \right]^{0.5} \left( \frac{2f_m u_m^3}{d} \right)^{0.4} \left( \frac{\rho_l}{\sigma} \right)^{0.6} - 0.725 \right\}^2 \quad (3.18)$$

where  $f_m$  is the mixture friction factor given by,

$$f_m = 0.046 \left( \frac{v_l}{u_m d} \right)^{0.2} \quad (3.19)$$

Note that  $u_m$  is the mixture velocity ( $u_m = u_{sg} + u_{sl}$ ), and  $v_l$  is the kinematic viscosity of the liquid phase.

For pipe diameters larger than  $d_T$ , a transition from bubble flow directly to churn flow is observed (Zabaras et al., 2013). A modified version of the classical model of Taitel et al. (1986) to the bubble-to-slug transition is used in this study to predict the bubble-to-churn flow transition. Omebere-Yari and Azzopardi (2007) modified Taitel et al.'s bubble-slug transition model (Taitel et al., 1986) by adjusting the critical voidage from 0.25 to 0.68. This value represents the maximum value for bubble flow observed in their experiments when a mixture of naphtha and nitrogen is tested in a 52 m high, 0.189 m (7.44 in) diameter vertical pipe at 20 and

90 bara (290 to 1,300 psia). This modified Omebere-Yari and Azzopardi (2007) transition model is given by the superficial gas velocity for the bubble-to-churn transition,

$$u_{sg,bc} = 2.13u_{sl} + 1.04 \left[ \frac{g(\rho_l - \rho_g)}{\rho_l^2} \right]^{0.25} \quad (3.20)$$

where churn flow occurs when  $u_{sg} \geq u_{sg,bc}$ , and the bubble flow occurs when  $u_{sg} < u_{sg,bc}$ .

### 3.1.5 Main Contributions of Proposed Model

This study proposes a new model for churn and annular flow regimes for vertical and near-vertical pipes, since it includes the term  $\sin\theta$  to the gravitational component in Equations (3.1) and (3.2). This model can be applied to two-phase flows in small and large pipe diameters, by modifying the correlations proposed by Jayanti and Brauner (1994) for the calculation of the interfacial friction factor,  $f_i$ , in Equation (3.9) by using Equations (3.910) to (3.14), and by the selection of correlations for the flow regime transitions (Equations (3.15) to (3.20)).

The study of Jayanti and Brauner (1994), which was originally developed only for churn flow conditions, was used as the basis of the churn flow model and extended to annular flow conditions. In addition to that, the work of Jayanti and Brauner (1994) was validated only for small pipe diameters, using an experimental data set for pipe diameter of 0.032 m (1.25 in), while this study validates the present model for large pipes diameters. Furthermore, the model of Jayanti and Brauner (1994) recommended the use of Jayanti and Hewitt (1992) method for the slug-to-churn flow regime transition, which was modified in the present study by the transition correlations presented in Section 3.1.4 depending on the pipe diameter. Besides that the model proposed by Jayanti and Brauner (1994) recommended the use of Equation (3.15) to estimate the transition from churn to annular flow. This study uses Equation (3.15) and Equation (3.16), depending on the pipe diameter, as described in Section 3.1.4.

Another main contribution in this study is the modification on the calculation of interfacial friction factor ( $f_i$ ) for churn and annular flow conditions. Jayanti and Brauner (1994), which was developed for churn flow regime only, suggested the use of different correlations to calculate  $f_{i,B}$  and  $f_{i,w}$  in Equation (3.9). In the present study,  $f_{i,B}$  is calculated using the correlation suggested by Alves (2014), and  $f_{i,w}$  is calculated without the classical assumption of thin films of Wallis (1969) for churn flow regime (as this regime is known to have a thick liquid film, particularly for large diameter pipes), while the assumption of thin film is used for annular flow. These modifications to Equation (3.9) have proven to provide significantly better results for the pressure gradient and liquid holdup predictions, as it is shown later in this study. Also, by using Equations (3.13) and (3.14), the model proposed has extended its application to annular flow regime.

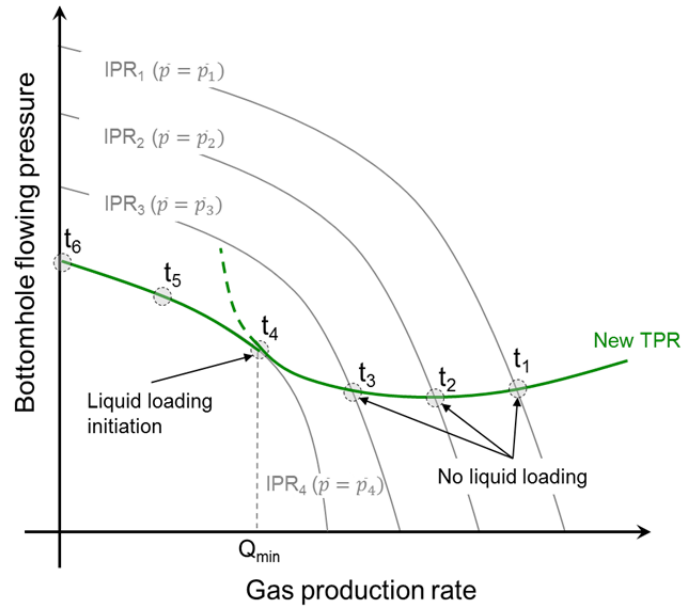
The model proposed in this study also avoids the use of additional empirical correlations for the liquid entrainment in the gas core for annular flow conditions, which is used in various modern models for annular flow regime. The addition of more empirical correlations can be understood as adding more uncertainty to the model for a wider range of conditions, as the empirical correlations should give reliable results only for the range of conditions tested.

### **3.2 Liquid Loading Initiation Model**

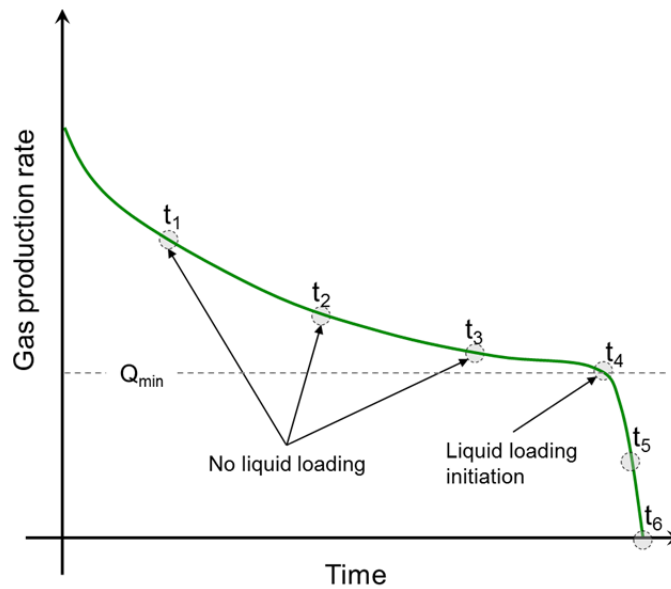
This study also proposes a model on the prediction of liquid loading initiation. This model uses the concept of nodal analysis, reservoir gas material balance in pseudosteady state conditions, and a new TPR model to represent the transient effects after liquid loading inception. In this study, liquid loading initiation is assumed to take place when the IPR is just tangent to the TPR curve, represented by  $Q_{min}$ , as shown in Figure 3.2a. The TPR in Figure 3.2a represents the concept of the new TPR proposed here.



When liquid loading initiates, the TPR no longer follows the path through the dash line, which is the usual shape of a TPR curve for gas-liquid two-phase flow in vertical and near-vertical pipes.



(a)



(b)

Figure 3.2 – Proposed nodal analysis technique to predict liquid loading: (a) the tangent between the IPR and TPR curves defines liquid loading initiation, and (b) gas production rate suddenly declines after time  $t_4$  as the reservoir cannot sustain steady-state two-phase flow for flow rates lower than  $Q_{min}$ .

According to the proposed model in this study, the TPR follows a new path when gas rates decrease from  $Q_{min}$ . This new TPR path follows the IPR curve for gas rates lower than  $Q_{min}$ , as shown as a bold curve in Figure 3.2a. For gas rates lower than  $Q_{min}$ , the bottomhole pressure suddenly increases and equals the reservoir pressure. Figure 3.2b shows the gas production rate depletion with time. After liquid loading is initiated, there is a sudden decrease in gas production rate, as the reservoir can no longer sustain the steady-state two-phase flow for flow rates lower than  $Q_{min}$ .

This model assumes steady-state flow conditions for the multiphase flow in the wellbore and pseudosteady state flow in the reservoir for times before liquid loading initiation ( $t < t_4$  in Figure 3.2a), due to the slow transient conditions. After liquid loading initiation is reached ( $t \geq t_4$  in Figure 3.2a), the model uses a pseudosteady state approach for the two-phase flow in the wellbore and steady-state condition for the reservoir (due to fast transient in the wellbore flow). This model describes liquid loading initiation and liquid buildup without the use of the Turner (1969) critical velocity concept (Equation (2.9)). Instead, the model proposed here uses the concept of nodal analysis and the tangent point between the IPR and TPR curves to predict liquid loading initiation.

The nodal analysis technique requires the selection of a model for the calculation of an IPR curve and a flow correlation for the calculation of the TPR curve. This study proposes the use of a conventional IPR curve for pseudosteady state conditions for the reservoir (Economides et al., 2013), and the use of the model proposed in this study for churn and annular flows in a wellbore for the estimation of the TPR curve (described in Section 3.1). The selection of the IPR and TPR correlations is further described in the next sections.

### 3.2.1 Reservoir Inflow Performance Model (IPR)

The reservoir model uses conventional gas inflow performance relationships. As liquid loading occurs in the late life of gas wells, pseudosteady state conditions can be assumed and non-Darcy effects can be neglected. Therefore, the IPR for the gas reservoir is calculated by the following expression:

$$q = J(\bar{p}^2 - p_{wf}^2) \quad (3.21)$$

where  $q_g$  is the production gas flow rate,  $J$  is the productivity index,  $\bar{p}$  is the average reservoir pressure,  $p_{wf}$  is the wellbore bottomhole flowing pressure.

To capture the transient decline in the gas flow rate, pseudosteady state change in the average reservoir pressure ( $\bar{p}$ ) can be obtained using reservoir material balance (Economides et al., 2013). A simple version of gas material balance is given by the following well-known expression,

$$\frac{\bar{p}_n}{\bar{z}_n} = \frac{p_i}{z_i} \left( 1 - \frac{G_{p_n}}{G_i} \right) \quad (3.22)$$

where  $p$  is the reservoir pressure,  $z$  is the gas compressibility factor,  $G_p$  is the cumulative production, and  $G_i$  is the initial gas-in-place. The subscript  $i$  means initial,  $n$  refers to the current time step, and the bar over the  $p$  and the  $z$  means average conditions. Based on the knowledge of the reservoir initial conditions, and on the current pressure and gas compressibility,  $G_{p_n}$  is calculated for each time step  $\Delta t$ , assuming production gas flow rate constant within each time step.

### 3.2.2 Tubing Performance Relationship (TPR)

The Gray (1974) correlation is the most widely used flow correlation to calculate pressure drop over the tubing for gas wells. This correlation was shown to predict pressure drop

accurately over a wide range of conditions in gas wells (Reinicke et al., 1987). However, as shown by Oudeman (1990), the Gray correlation may present problems for low-pressure, low-gas rate wells. Oudeman showed an example where the Gray correlation underpredicted the actual pressure gradient by 27%, for a low-gas rate well. As liquid loading occurs in the late life of gas wells it is important to develop and test improved models for low-pressure, low-rate wells.

This study uses the new wellbore model proposed in this study (see Section 3.1), which is based on a mechanistic model for gas-liquid annular and churn flow regimes. This model is described in Section 3.1, and it is validated with laboratory and field data over a wide range of conditions, including low pressure low gas rate flows. This validation is presented and discussed in Section 4.1. The accuracy of the model described in Section 3.1 for prediction of pressure gradient was compared to measured data using natural gas-oil and air-water mixtures, for pipe diameters ranging from 0.032 m (1.25 in) to 0.28 m (11 in), and pressures from 1 bara (15 psia) to 614 bara (8,900 psia). When using field data, the absolute average errors for the TPR model presented in this study (Section 4.1) on the prediction of bottomhole pressure, and pressure profile along the wellbore, stayed within the range of 6%. More importantly, this TPR model showed a superior accuracy in prediction of the laboratory measured pressure drop with varying gas flow rate when compared to other widely used models for TPR estimation. Section 4.2 shows that even though some TPR models show high accuracy for a wide range of conditions, if the same models have inferior accuracy for low gas rates (for instance, the case of the Gray (1974) correlation), they may not be desirable for prediction of liquid loading in gas wells.

After the selection of the correlations for the IPR and TPR simulations, the nodal analysis can be performed in order to find the liquid loading critical rate ( $Q_{min}$ ). Once  $Q_{min}$  is reached, (time  $t_4$  in Figure 3.2a), a sudden decrease in gas flow rate leads the liquid film to start falling,

which buildups in the bottom of the wellbore. This phenomenon represents pseudosteady state changes in the fluid flow in the vertical or near-vertical tube. The study of Waltrich et al. (2015a) shows experimentally that a new steady-state flow condition can be re-established in the wellbore by a larger liquid holdup front flowing upwards from the bottom to the top of the tube, if there is continuously liquid-and-gas injection from the reservoir.

The bottomhole pressure for times after  $t_4$  is calculated using a similar approach as proposed by Dousi et al. (2006). The changes in the friction component (left term of the right hand-side of Equations (3.1) and (3.2)) are neglected since the gravitational effects at this point are much larger than the frictional effects (due to the low-gas rates). Thus, only the increase in bottomhole pressure due to the increase in the liquid column (hydrostatic pressure) is considered. Then, the transient bottomhole flowing pressure for gas flow rates lower than  $Q_{min}$  ( $t_5$ ) is calculated using the following expression,

$$p_{wf,t_5} = p_{wf,t_4} + \frac{q_l}{A}(t_5 - t_4)\rho_l g \sin\theta \quad (3.23)$$

where  $p_{wf,t_5}$  is the bottomhole flowing pressure at a time  $t_5$ , and  $p_{wf,t_4}$  is the bottomhole flowing pressure at liquid loading initiation (at time  $t_4$ ),  $q_l$  is the constant liquid rate inflow,  $A$  is the cross-sectional area of the pipe, and  $t_5$  is any time after liquid loading initiation, but before the well stops flowing completely (time  $t_6$ ).

The gas production keeps decreasing as the bottomhole pressure increases until it reaches the average reservoir pressure ( $t_6$  in Figure 3.2a), when the well ceases production. In order to calculate the time the wellbore stops flowing after it starts suffering from liquid loading, Equation (3.24) is used, which is the rearrangement of Equation (3.23) replacing  $t_5$  by  $t_6$ :

$$t_6 = (p_{wf,t_6} - p_{wf,t_4}) \frac{A}{\rho_l g q_l \sin\theta} + t_4 \quad (3.24)$$

where  $p_{wf,t_6}$  is the bottomhole flowing pressure when well stop flowing, at time  $t_6$ . This is the pressure when gas production rate is zero, which is the same pressure as the given reservoir pressure when the tangent of the IPR curve is the same as the TPR curve (see Figure 3.2a).

Liquid holdup from time  $t_1$  up to time  $t_4$  (right before liquid loading initiation) is usually estimated from the solution of Equations (3.1) and (3.2). After time  $t_4$ , this study proposes that the liquid holdup at time  $t_i$  ( $H_{l,t_i}$ ) can be calculated by

$$H_{l,t_i} = H_{l,t_4} + \frac{\frac{q_l}{A}(t_i - t_4)}{MD} \quad (3.25)$$

where  $H_{l,t_4}$  is the liquid holdup at the time of liquid loading initiation,  $MD$  is the wellbore measured depth, and  $t_i$  is any time after liquid loading initiation (it can be replaced by  $t_5$  or  $t_6$ ).

Once the well stops flowing, tubing wellhead pressure increases, and the liquid column in the bottom of the wellbore starts to be injected back into the formation (Dousi et al., 2006). A new production cycle is re-started when the liquid holdup in the wellbore reaches the same level at liquid loading initiation and wellhead pressure is lowered, assuming a continuous liquid injection from the reservoir to the wellbore.

## 4. Model Validation, Results and Discussions<sup>1,2</sup>

This chapter is divided into two main sections. The first section shows the validation of the model proposed in this study for churn and annular flow regimes, using laboratory and field data. Simulations using PIPESIM software (PIPESIM, 2013) for different correlations are also presented. All the simulations were performed for each data point of the experimental and field data selected for this study. The second section of this chapter discusses the validation and results on the prediction of liquid loading initiation based on a set of field data for 10 wells. It also compares the prediction of liquid loading initiation using the current models available in the literature (as described in Section 2.2).

### 4.1 Churn and Annular Flow Modeling Validation Results

The accuracy of the proposed model is compared with laboratory data (using databases from Owen, 1986; Van der Meulen, 2012; Yuan et al., 2013; Zabararas et al., 2013; Skopich et al., 2015), and field data (using the data set from Fancher and Brown, 1963; Reinicke et al., 1987). The data collected from these different studies includes a wide range of pipe diameters of 0.0318 to 0.2794 m (1.252 to 11 in) and pressures of 1 to 613 bara (15 to 8,900 psia), in both air-water and oil-natural gas systems. Also, different correlations found in the PIPESIM software (PIPESIM, 2013), as well as in the previous model of Jayanti and Brauner (1994), were used to simulate this set of data and to compare their performance against the model proposed in this study.

---

<sup>1</sup>Section 4.1 of this chapter previously appeared as E. Pagan, W. C. Williams, S. Kam, P. J. Waltrich, Modeling Vertical Flow in Churn and Annular Flow Regimes in Small- and Large-Diameter Pipes, Paper Presented and Published at BHR Group's 10th North American Conference on Multiphase Technology 8-10th June 2016. It is reprinted by permission of Copyright © 2016 BHR Group. See Appendix for more details.

<sup>2</sup>Section 4.2 of this chapter previously appeared as Erika V. Pagan, Wesley Williams, and Paulo J. Waltrich, A Simplified Transient Model to Predict Liquid Loading in Gas Wells, Paper SPE-180403-MS presented at the SPE Western Regional Meeting held in Anchorage, Alaska, USA, 23-26 May 2016. It is reprinted by permission of Copyright 2016, Society of Petroleum Engineers Inc. Copyright 2016, SPE. Reproduced with permission of SPE. Further reproduction prohibited without permission. See Appendix for more details.

#### 4.1.1 Comparison with Laboratorial Data

A literature search identified five laboratory data sets including experimental data with pipe diameters ranging from 0.032 m (1.25 in) to 0.279 m (11 in), using air-water mixtures at the conditions close to the atmospheric pressure.

Figure 4.1 and Figure 4.2 present the comparison between simulation results from the model in this study and experimental data obtained by Skopich et al. (2015) in vertical pipes of diameters 0.0508 m (2 in) and 0.1016 m (4 in). The modeling results of Ansari et al. (1994) and OLGA (2000) are also provided by Skopich et al. (2015). In this study, simulation results using Duns and Ros (1963), Gray (1974), and Jayanti and Brauner (1994) models are added. Since Jayanti and Brauner (1994) method was proposed only for churn flow regime, the simulation results are not included for this model for flow regimes different than churn flow.

Figure 4.1 presents the pressure gradient and liquid holdup at the diameter of 0.0508 m (2 in), and superficial liquid velocities of 0.01 and 0.05 m/s. The model in this study predicts annular flow at superficial gas velocities higher than 20 m/s, and churn flow regime for lower gas velocities. This flow regime transition shows a reasonable agreement with the experimental flow regime transition observations of Skopich et al. (2015). Figure 4.1 shows that the model proposed in this study also has a good agreement in terms of pressure gradient at pipe diameter of 0.0508 m (2 in), for both superficial liquid velocities, and for the wide range of superficial gas velocities tested. Since this study is based on Jayanti and Brauner (1994) model, it is not surprising that both models present similar results for churn flow and small diameter conditions, as the models from the latter authors was originally developed for small diameter pipes. The other models (with exception of Duns and Ros (1963) model) showed a good prediction of pressure gradient only for annular flow, but seem to fail to capture the trend for churn flow (e.g.,



for superficial gas velocities lower than 20 m/s). This mismatch is likely because these models do not include a separate model for the churn flow regime. Instead, they try to simulate churn flow with either a slug flow model or extending the annular flow regime to lower superficial gas velocities.

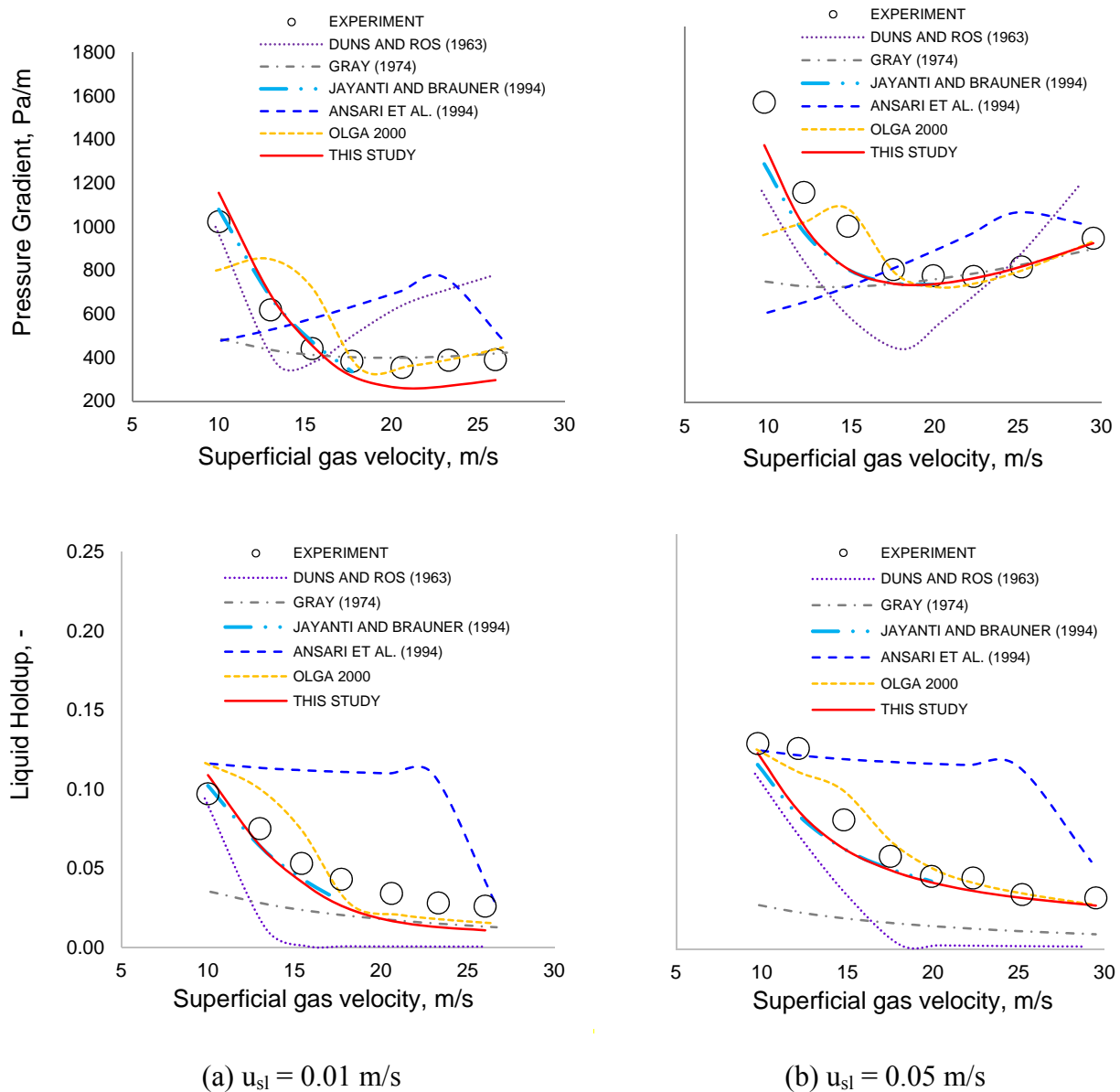


Figure 4.1 - Comparison between model and experimental results in terms of pressure gradient and liquid holdup (data from Skopich et al., 2015), for 0.0508 m (2 in) pipe diameter and superficial liquid velocities of (a) 0.01 m/s, and (b) 0.05 m/s.

In the other hand, Duns and Ros (1963) correlation have a different result, presenting reasonable predictions for churn regime, however, over predicting pressure gradient for annular flow conditions.

Figure 4.1 also shows the experimental liquid holdup obtained by Skopich et al. (2015) for a 0.0508 m (2 in) pipe diameter. Overall the model proposed in this study exhibits a better performance in terms of liquid holdup prediction. The model proposed in this study, Jayanti and Brauner (1994), and OLGA (2000) are the only models predicting the trends and magnitudes of liquid holdup for all the entire range of superficial gas velocities. The model of Duns and Ros (1963) shows a reasonable match for low superficial velocities, under predicting values of holdup when increasing superficial gas velocities. Jayanti and Brauner (1994) correlation shows similar results to this study for churn flow regime. Simulation results for annular flow regime is not included for Jayanti and Brauner (1994), as the original work of these authors do not include a separate model for annular flow.

For intermediate pipe diameters, the model in this study also shows a reasonable performance. Figure 4.2 presents the experimental pressure gradient and liquid holdup for a pipe diameter of 0.1016 m (4 in). The model proposed in this study shows an acceptable prediction of the experimental pressure gradient values and trend for the entire range of superficial gas velocities tested. The simulation results from Jayanti and Brauner (1994) for larger diameter show over predictions for the experimental pressure gradient when compared to the model proposed in this study. From Figure 4.2, it is possible to note that this study improved the model of Jayanti and Brauner (1994) for churn flow regime, decreasing the over prediction of pressure gradient for intermediate pipe diameters. Duns and Ros (1963), Gray (1974), Ansari et al. (1994), OLGA (2000), and the model in this study show a good agreement for the annular flow

regime (e.g., superficial gas velocities higher than 15 m/s). Duns and Ros (1963), Jayanti and Brauner (1994) and the model proposed in this study reasonably captures the trend of the experimental pressure gradient for the churn flow region (superficial gas velocities lower than 15 m/s).

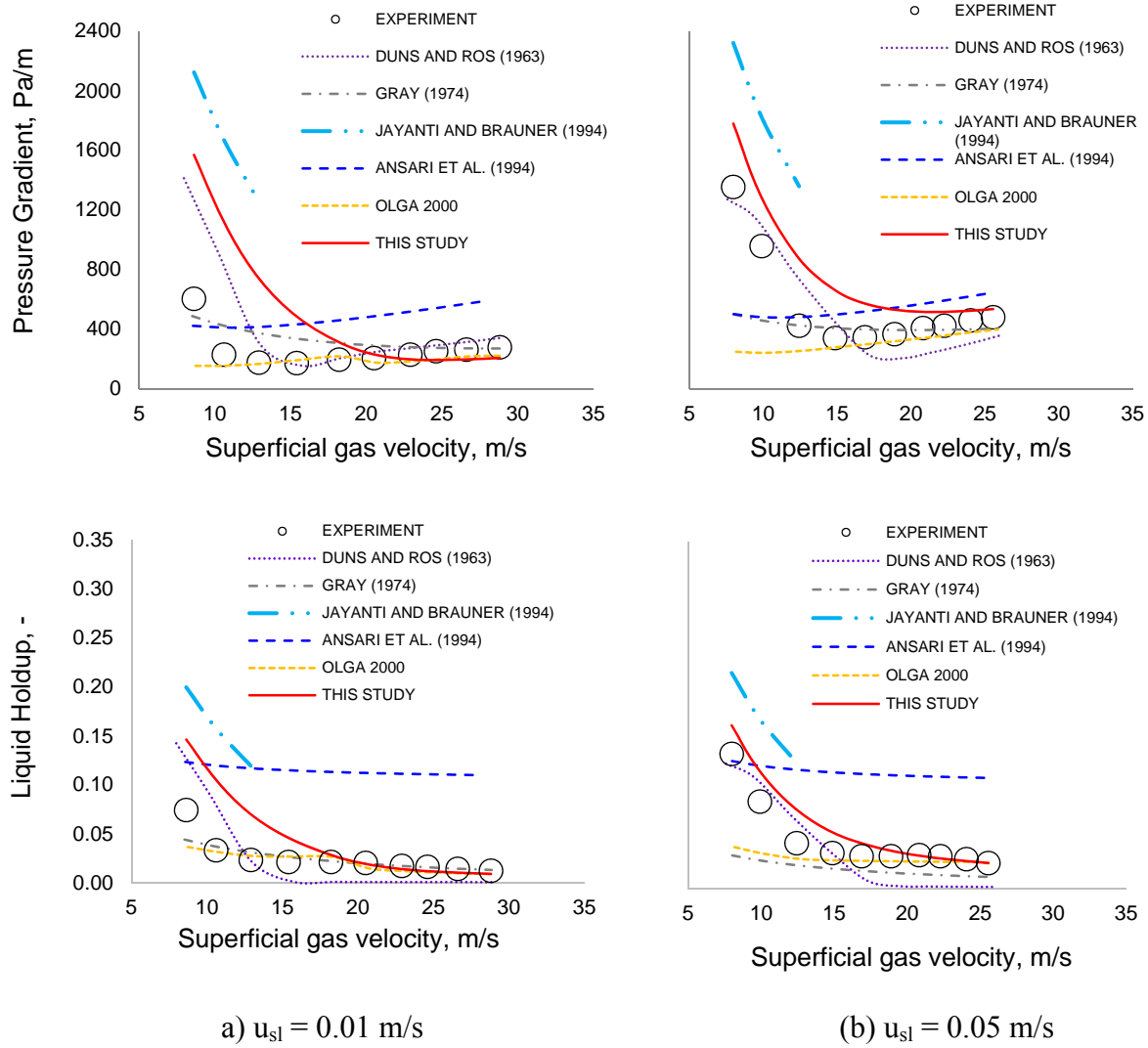


Figure 4.2 - Comparison between model and experimental results in terms of pressure gradient and liquid holdup (data from Skopich et al., 2015), for 0.102 m (4 in) pipe diameter and superficial liquid velocities of (a) 0.01 m/s and (b) 0.05 m/s.

Figure 4.2 also shows the measurements for liquid holdup for pipe diameter of 0.1016 m (4 in). Ansari et al. (1994) predicts liquid holdup significantly higher than the experimental data.

All the other models showed accuracy to the liquid holdup prediction similar to the results for pressure gradient.

Figure 4.3 presents the experimental pressure gradient for a 0.127 m (5 in) pipe diameter. The model proposed in this study again shows a good prediction of experimentally measured pressure gradient values and trend. Overall it shows a better performance when compared to the other models tested for matching the experimental pressure gradient data for both superficial liquid velocities. For both superficial liquid velocities presented in Figure 4.3, churn flow regime was predicted to happen from low superficial gas velocities up to 9 m/s, when the flow regime changed to annular.

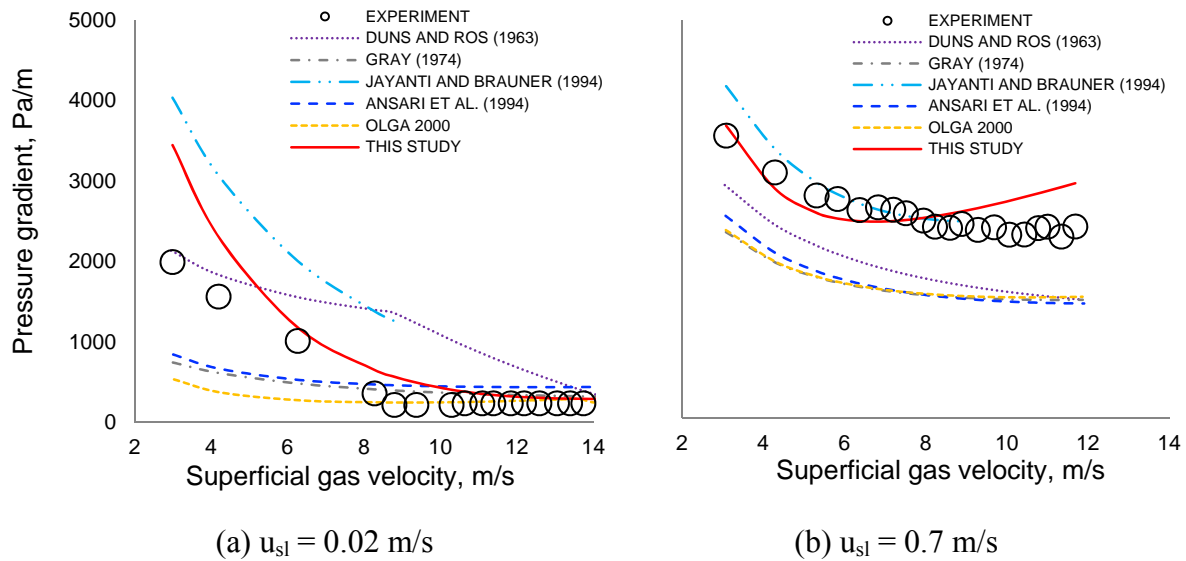


Figure 4.3 - Comparison between model and experimental results in terms of pressure gradient (data from Van de Meulen, 2012), for 0.127 m (5 in) pipe ID, and liquid superficial velocities of (a) 0.02 m/s and (b) 0.7 m/s.

For larger pipe diameters, the model proposed in this study also shows good performance. Figure 4.4 presents the experimentally measured pressure gradient for a 0.2794 m (11 in) pipe diameter. Again, the model proposed in this study shows a good prediction of pressure gradient for the entire range of superficial gas velocities. All the experimental values

presented in the two graphs of Figure 4.4 are estimated to be in churn flow regime, according to the correlations for flow regimes transition used in this study.

Figure 4.5 shows the comparison between experimental and calculated results for all models evaluated in this study on the prediction of the experimental pressure gradient. Figure 4.5a includes the comparison for all the values of pressure gradient (354 data points), for five different data sets previously published and collected for this study (Owen, 1986; Van der Meulen, 2012; Yuan et al., 2013; Zabaras et al., 2013; Skopich et al., 2015).

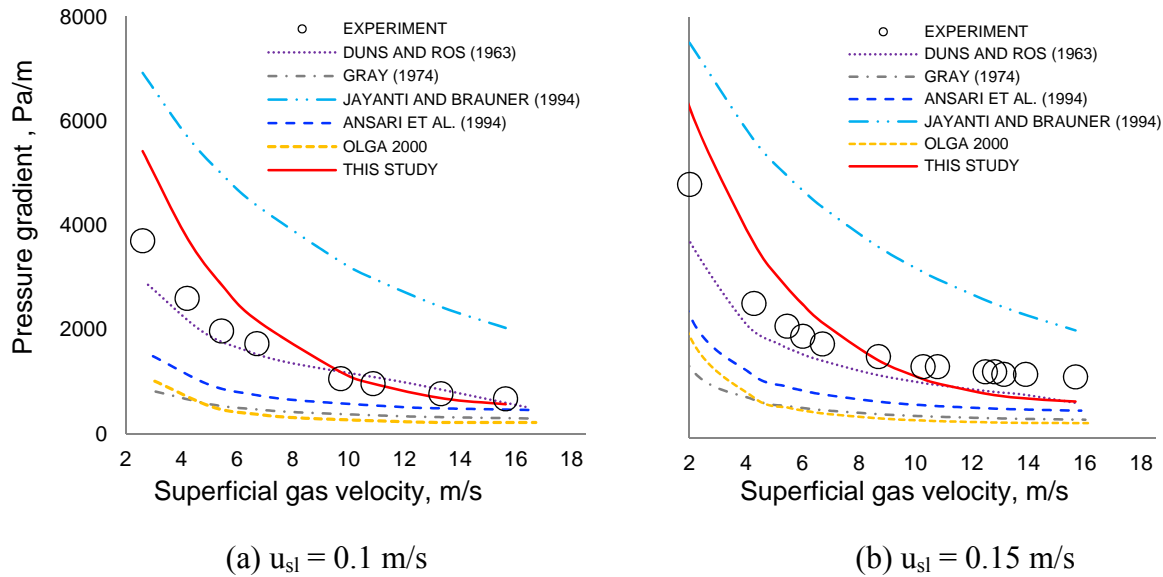
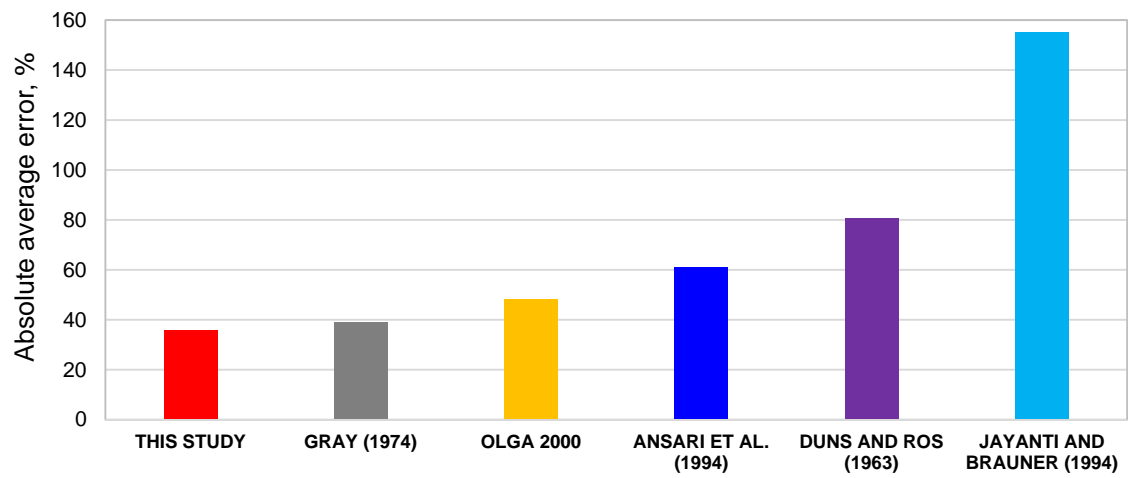


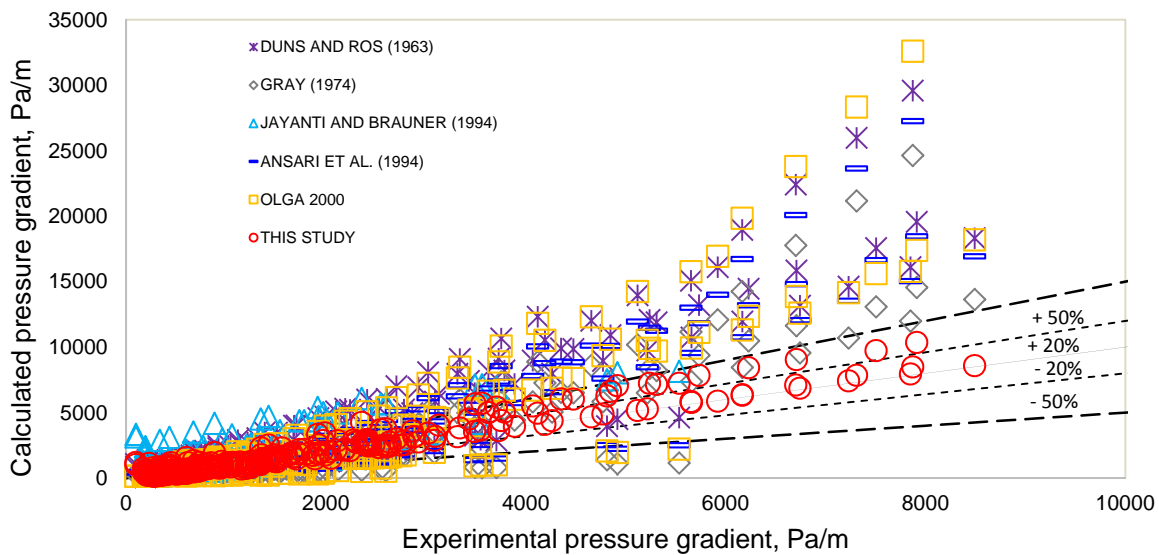
Figure 4.4 - Comparison between model and experiments results in terms of pressure gradient (data from Zabaras et al., 2013) for 0.279 m (11 in) pipe ID, and liquid superficial velocities of (a) 0.03 m/s and (b) 0.15 m/s.

Figure 4.5 shows that this study has an overall better performance when estimating the pressure gradient for the experimental data when compared to the other flow models tested, presenting an absolute average error of 36%. The best performance is followed by the results of Gray (1974) correlation, OLGA (2000), Ansari et al. (1994) model, Duns and Ros (1963), and Jayanti and Brauner (1994) method. Gray's (1974) absolute average error is close to the error for the model proposed in this study. However, this study captures the trend of the pressure gradient

more accurately, for all the values of superficial gas velocities and diameters (see Figure 4.1 to Figure 4.4). This is very important when applying a wellbore model to predict liquid loading initiation based on the approach proposed in this study (see Sections 3.2 and 4.2). The better performance for the model proposed in this study can be attributed to the fact that this model has a dedicated model for churn flow and the modifications added to the original churn flow model of Jayanti and Brauner.



(a)



(b)

Figure 4.5 – (a) Absolute average error and (b) comparison between experimental and calculated pressure gradient for models used in this study.

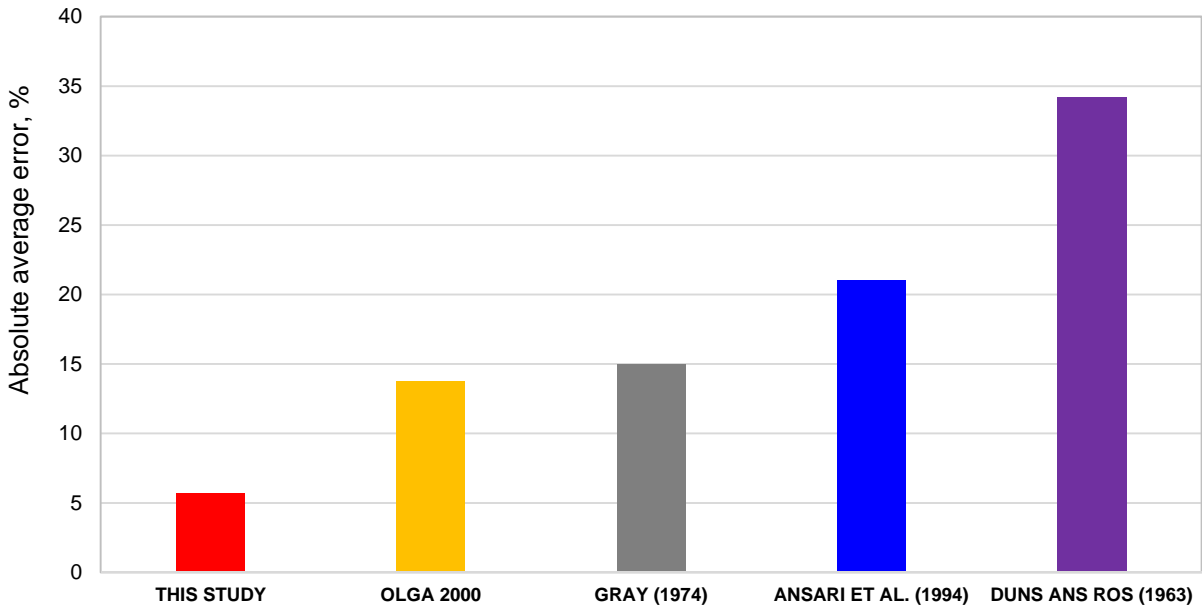
#### 4.1.2 Comparison with Field Data

A search in the literature is also carried out to find available field data which includes wellbore pressure for intermediate and high GLRs, and small- and large-diameter vertical and near-vertical pipes. The two field data sets of Fancher and Brown (1963) and Reinicke et al. (1987) are identified with pipe diameters ranging from 0.0508 m (2 in) to 0.101 m (3.976 in), tubing inclinations between 0 and 8.2 degrees, GLR between 94 m<sup>3</sup>/m<sup>3</sup> and 250,000 m<sup>3</sup>/m<sup>3</sup> (525 scf/bbl and 1.4 MMscf/bbl), oil-water-natural gas mixtures, and pressures up to 612 bara (8,900 psia).

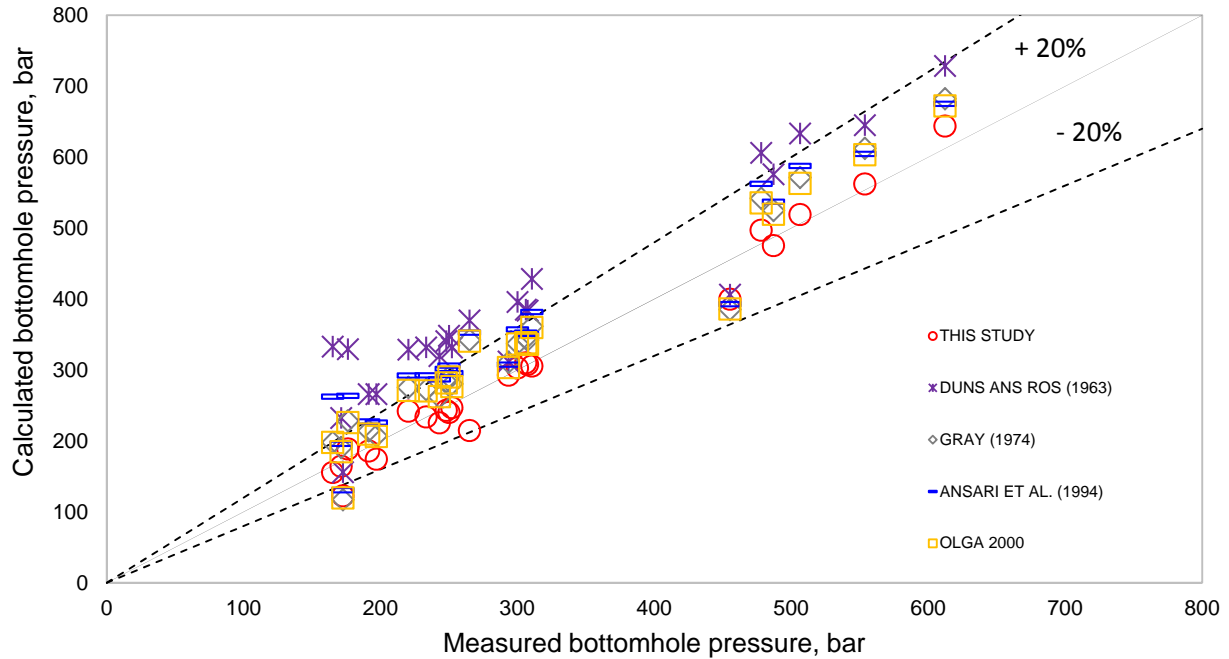
The fluid properties required for the calculation as an input for the model in this study assumes black oil correlations for the oil properties, and real gas law for natural gases for the gas properties (Brill and Mukherjee, 1999). The specific gravities of oil, gas and water are used as input as given by the data set of Fancher and Brown (1963) and Reinicke et al. (1987). The fluid temperature is assumed to change linearly from the bottomhole to the wellhead, using the temperature measured at those two locations.

Figure 4.6 presents the prediction for field measured wellbore bottomhole pressure for Reinicke et al. (1987) database, which most wells have pipe diameters around 0.101 m (3.976 in). Out of 26 wells from their database, two wells are predicted to be under bubble flow conditions (using Equation (3.20)), and thus less relevant to this study. These two wells are not included in Figure 4.6. Out of the 24 wells selected, the simulation results predicted the bottomhole pressures of 23 wells within  $\pm 20\%$  deviation from the measured values. All 24 wells are predicted within the deviation range of  $\pm 30\%$  (Figure 4.6b). The absolute average error including all 24 wells is only 6% (Figure 4.6a). Figure 4.6a also presents the absolute average

error for the simulation of the 24 wells of Reinicke et al. (1987) using the flow correlations of Duns and Ros (1963), Gray (1974), Ansari et al. (1994), and OLGA (2000).



(a)



(b)

Figure 4.6 – (a) Absolute average error, and (b) calculated and measured bottomhole pressure for the field database of Reinicke et al. (1987), for wells having tubing diameters around 0.101 m (3.976 in).



The model proposed in this study resulted in an absolute average error much lower than the other correlations tested. The model of Jayanti and Brauner (1994) was not used to simulate this field data set since the wells were not only flowing under churn flow regime. It is clear to conclude from Figure 4.6 that the model proposed in this study has significantly more accurate for churn and annular flow in wellbore or larger diameter, when compared to the other widely used models.

Figure 4.7 shows the comparison between the model and field data of Fancher and Brown (1963) for pressure profile along the wellbore, and for smaller tubing diameters (0.05 m – or 2 in). In addition, it also shows the flow regimes as predicted by the model proposed in this study. Figure 4.7 shows that the model proposed here has an excellent agreement with pressure profile for the field data of Fancher and Brown (1963). This database includes 20 cases for different oil rates and GLR. Twelve cases are selected from their database because they are predicted to have churn or annular flow regimes (as predicted by the model) at least in a certain portion of the wellbore.

Interestingly, the model proposed in this study predicts, with reasonable accuracy, the pressure gradient for slug flow conditions, even though it was originally developed only for churn and annular flow regimes. These results indicate that the model proposed in this study should potentially be used to estimate slug flow in conditions near to the churn flow regime. However, further investigations should be carried out before this statement can be confirmed.

Figure 4.8a presents the absolute average error for the simulation of the 12 wells of Fancher and Brown (1963) using the model proposed in this study, as well as the correlations of Duns and Ros (1963), Gray (1974), Ansari et al. (1994), and OLGA (2000).

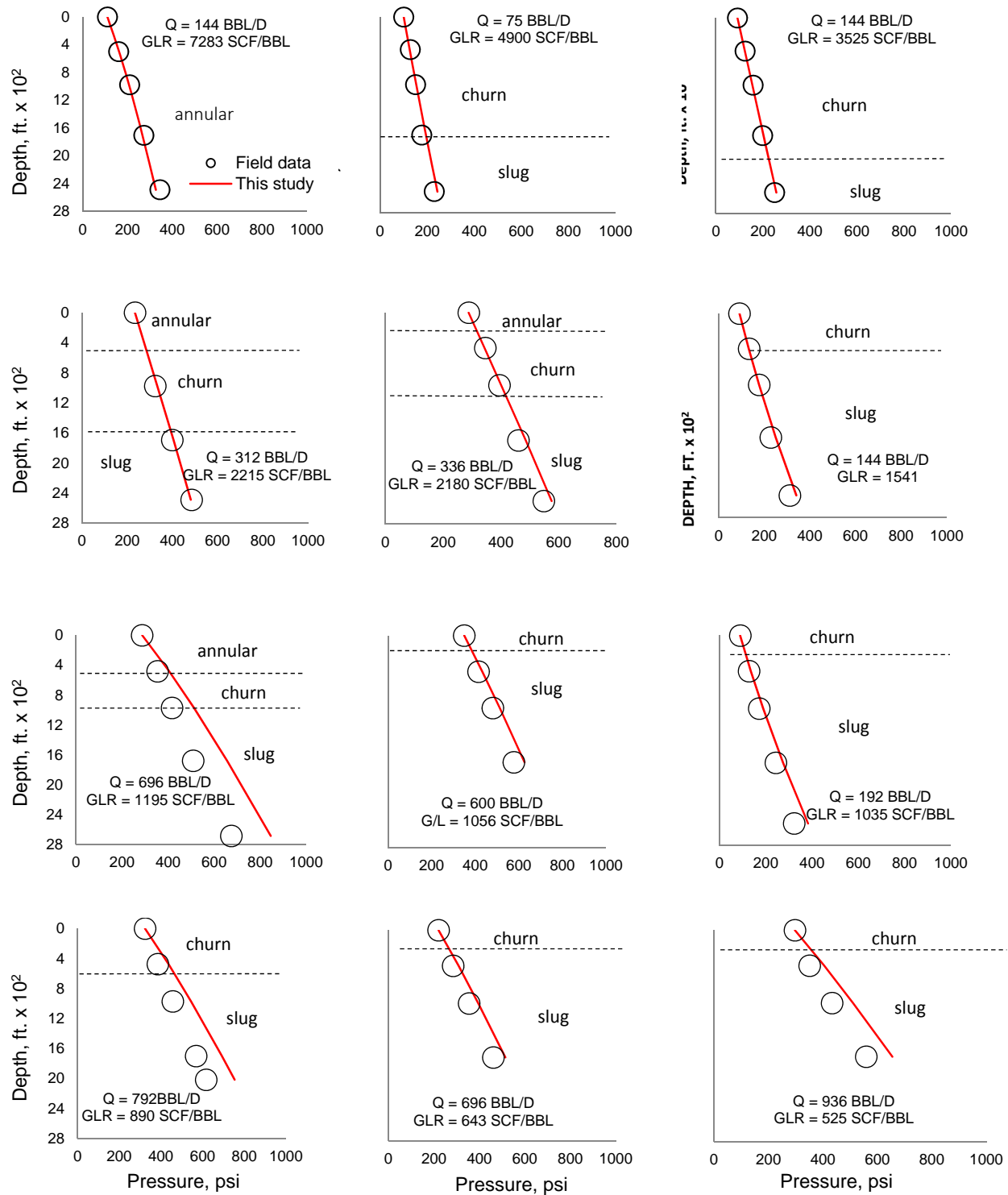
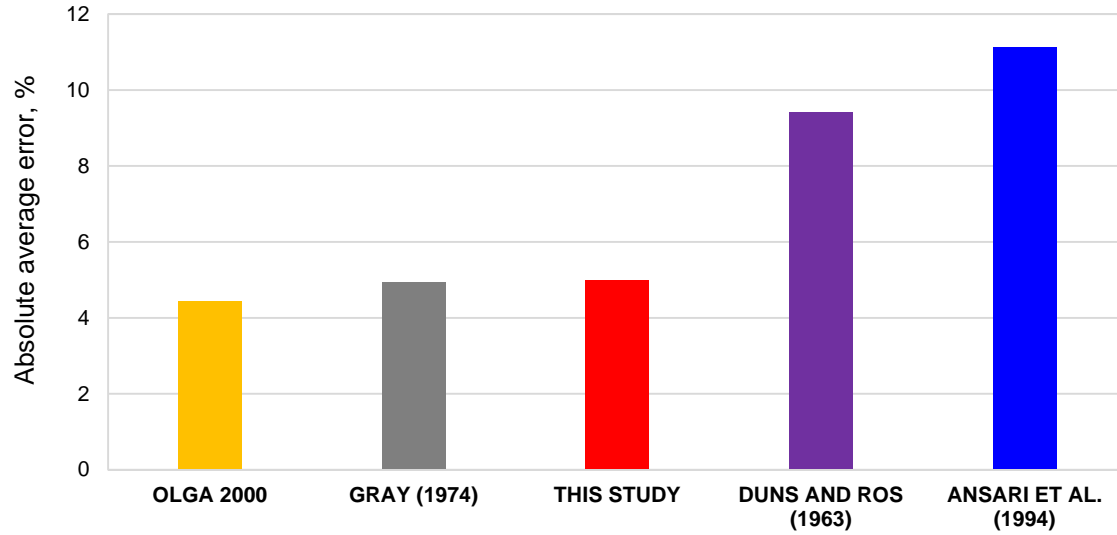
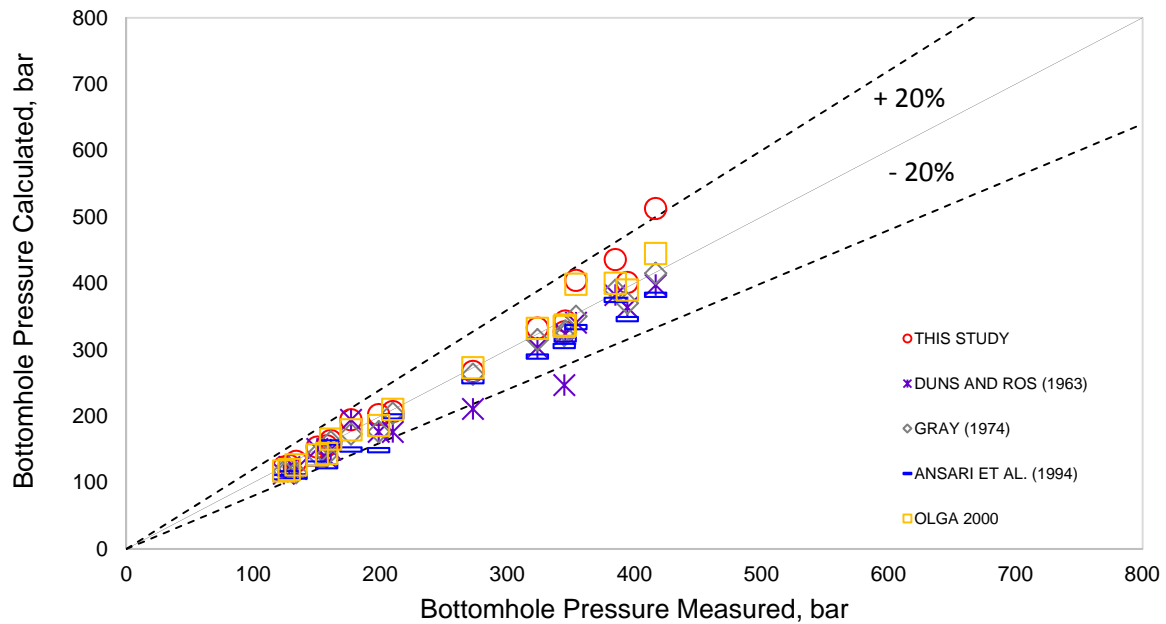


Figure 4.7 - Comparison between simulation results using the model proposed in this study and measured wellbore pressure profile (field data from Fancher and Brown, 1963). Circles represent the measured pressures and continuous lines are the simulated pressures. Dash lines represents the depth at which a flow regime transition happened based on the simulation.

Figure 4.8a shows that the absolute average error for the estimated pressure using the model proposed in this study for all the 12 wells was only 5%.



(a)



(b)

Figure 4.8 - (a) Absolute average error, and (b) calculated and measured bottomhole pressure for the field database of Fancher and Brown (1963), for wells having tubing diameters around 0.0508 m (2 in).

OLGA (2000) presented the overall best estimation for the data set of Fancher and Brown (1963), but its accuracy is essentially the same as the model proposed in this study. Ansari et al. (1994) and Duns and Ros (1963) present larger errors compared to the other models. Nevertheless, all flow model tested presented an absolute average error under 20% for this database with smaller tubing diameters. The model of Jayanti and Brauner (1994) was not used to simulate this field data set since the fluids in these wells were not only flowing in churn flow regime.

#### **4.2 Liquid Loading Modeling Validation and Result Discussions**

There are a few field data sets available in the open literature regarding liquid loading in gas wells. To the knowledge of the author, the most cited data sets are presented in Turner et al. (1969), Coleman et al. (1991), and Veeken et al. (2010). However, from these three widely used field data sets for liquid loading, the only one that includes enough information about wellbore and reservoir is the data set of Veeken et al. (2010). More importantly, the latter authors describe in details on how they have defined wells under liquid loading conditions. These authors have defined the minimum flow rate (critical rate) just before the well ceases production, as shown in Figure 4.9.

As liquid loading is a “field term” and can be interpreted differently by different engineers, it is very important to clearly define liquid loading conditions for an appropriate validation of the model. In addition to that, Veeken et al. (2010) also stated that they have only considered wells with acceptable quality flow measurement ( $\pm 20\%$ ). However, one of the drawbacks of the data set published by Veeken et al. (2010) is the non-disclosure of the production data for condensate or water flow rates. As liquid rates are usually low for gas wells, a fix water rate of  $7.9 \text{ m}^3/\text{D}$  ( $50 \text{ bbl/D}$ ) is assumed here for all wells in Veeken et al. (2010) database. This value of condensate or

water rates is a good approximation of the averages rates published by Turner et al. (1969), Reinicke et al. (1987), and Coleman et al. (1991).

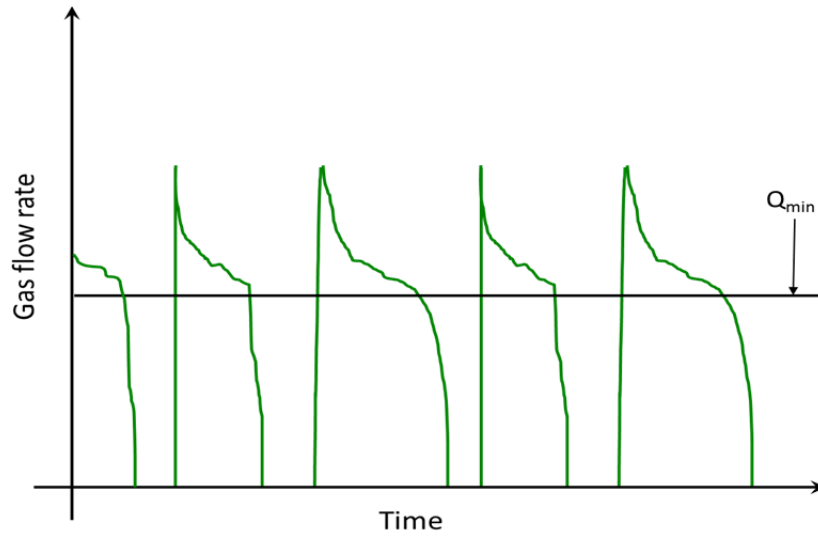


Figure 4.9 – Example on how Veeken et al. (2010) have defined the minimum gas flow ( $Q_{min}$ ) that represents the liquid loading initiation.

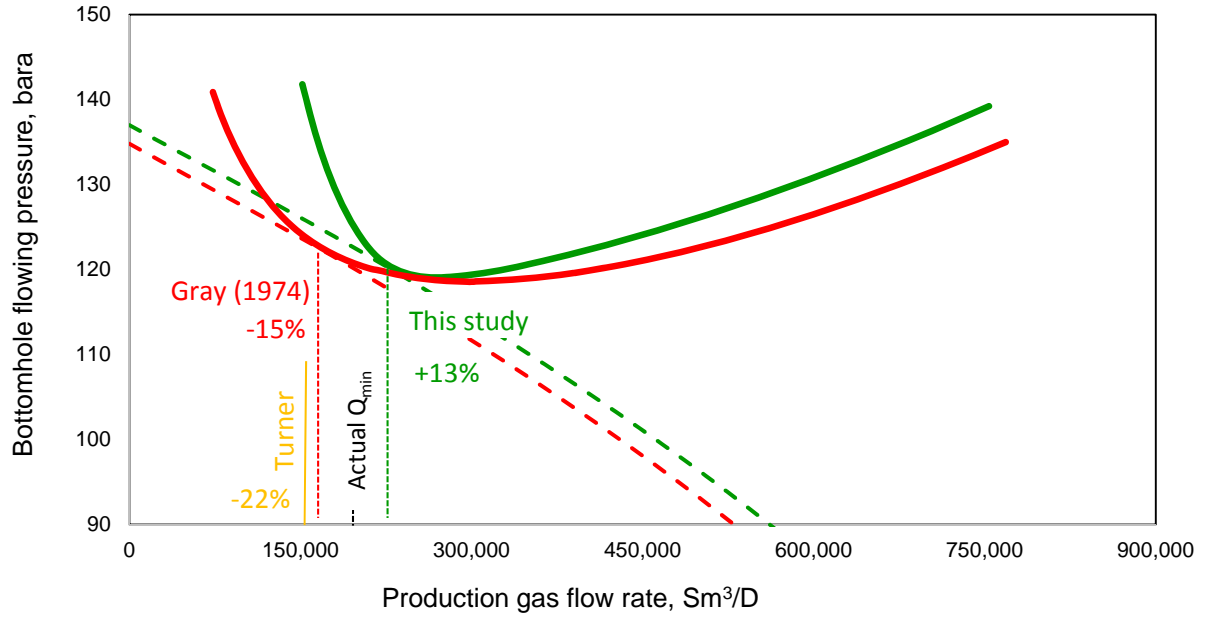
Out of sixty-six wells, ten wells were selected from Veeken et al. (2010) data set.

Table 1 presents the information for the ten wells selected. As the TPR model described in this study (Section 3.1) is only valid for vertical and near-vertical wells (up to 15 degrees of deviation), the selection of wells from this data set only included the wells with deviations ranging from 0 to 15 degrees. In addition to using field data to validate the approach proposed here to estimate liquid loading initiation, the flow model of Gray (1974) is also selected as TPR to evaluate the improvements on the prediction of liquid loading initiation when compared to the TPR model proposed in this study (Section 3.1). Turner's critical velocity concept given by Equation (2.9) is also evaluated.

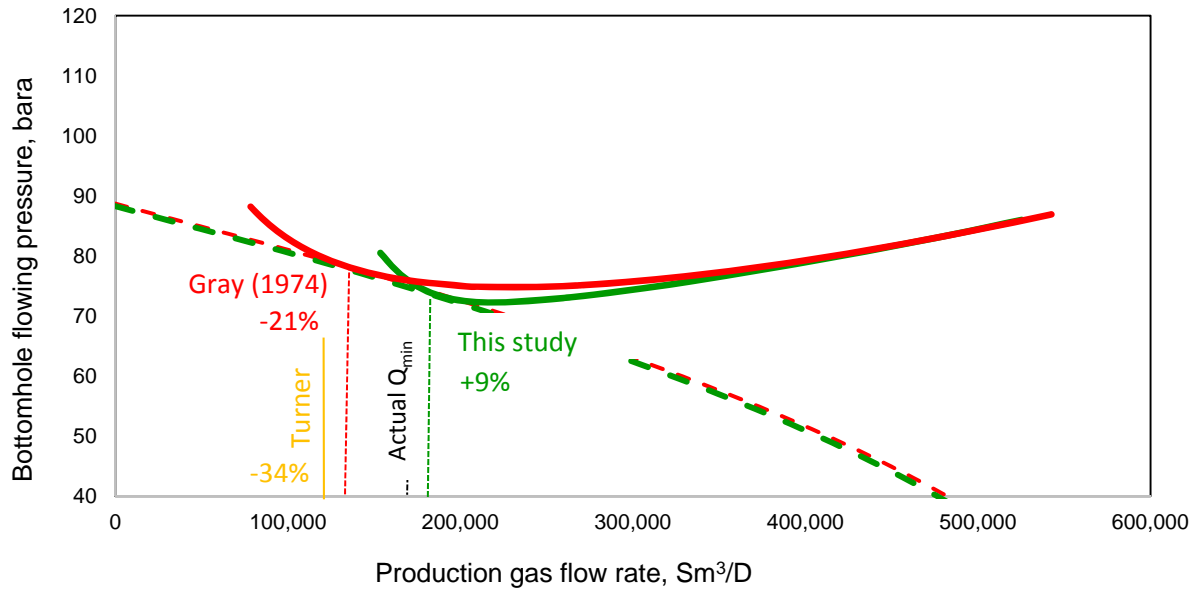
Figure 4.10 shows two examples to explain how the method proposed in this study was validated with the field data of Veeken et al. (2010). The latter authors measured minimum production flow rate that was correlated to liquid loading initiation ( $Q_{min}$ ).

Table 1 – Liquid loading data set for vertical and near-vertical gas wells published by Veeken et al. (2010).

Wellbore geometry					Reservoir and fluid properties		Production data			
							Wellhead		Bottomhole	
Well	MD (m)	TVD (m)	ID (in.)	Dev. (deg.)	Gas SG (-)	$J$ ( $\text{e}^3\text{Sm}^3/\text{D}/\text{bar}^2$ )	Pressure (bara)	Temperature ( $^{\circ}\text{C}$ )	Temperature ( $^{\circ}\text{C}$ )	$Q_{min}$ ( $\text{Sm}^3/\text{D}$ )
5	2,000	2,000	2.99	90	0.59	0.091	6	16	52	26,000
27	4,120	4,120	4.28	90	0.59	0.019	98	50	158	200,000
28a	4,120	4,120	4.28	90	0.59	0.053	85	50	158	200,000
28b	4,120	4,120	4.28	90	0.59	0.077	50	73	158	170,000
29	4,120	4,120	4.28	90	0.59	0.060	85	50	158	180,000
7	2,060	2,000	2.87	76	0.59	0.091	5.5	16	52	24,000
21	3,445	3,350	4.41	77	0.63	0.035	15	62	115	100,000
29a	3,130	3,025	6.09	75	0.61	0.909	46	75	120	530,000
29b	3,130	3,025	6.09	75	0.61	0.909	34	69	120	390,000
52	2,660	2,570	6.09	75	0.65	0.455	91	53	80	737,000



(a)



(b)

Figure 4.10 – Examples on how the method of using IPR tangent to TPR curve was validated with the minimum production flow rate for wells: (a) 28a, (b) 28b in Veeken et al. (2010) database. The figure also shows the results for the prediction of liquid loading initiation using the droplet model of Turner et al. (1969).

The model proposed here calculated this minimum production rate using nodal analysis, with different correlations to estimate the TPR curve (correlation proposed in this study and Gray

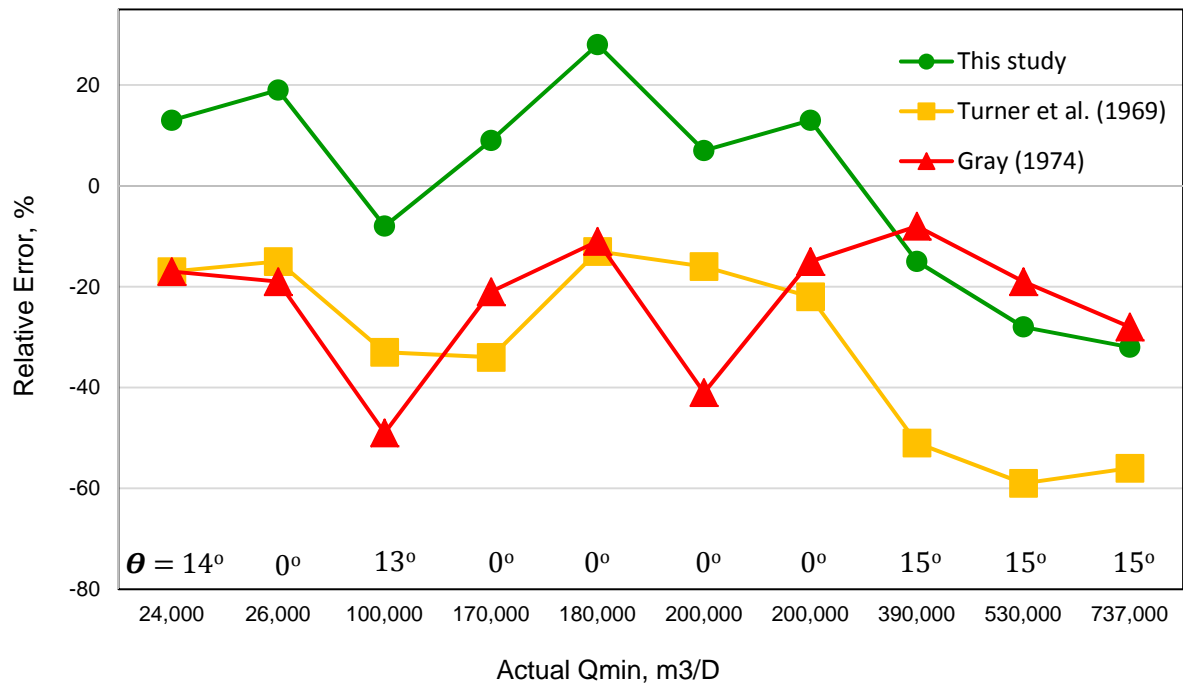
(1974) correlation). Liquid loading was estimated to be initiated when the IPR curve was tangent to the TPR curve.

The value of gas rate when the IPR is tangent to the TPR curve defines the minimum gas rate ( $Q_{min}$ ), which defines when the gas well starts suffering from liquid loading. Figure 4.10a and b also present the estimation of the minimum gas rate calculated by the droplet model of Turner et al. (1969). The results are shown in these figures in terms of percentage error from the models estimation to the actual field data of liquid loading initiation (actual  $Q_{min}$ ) as presented by Veeken et al. (2010).

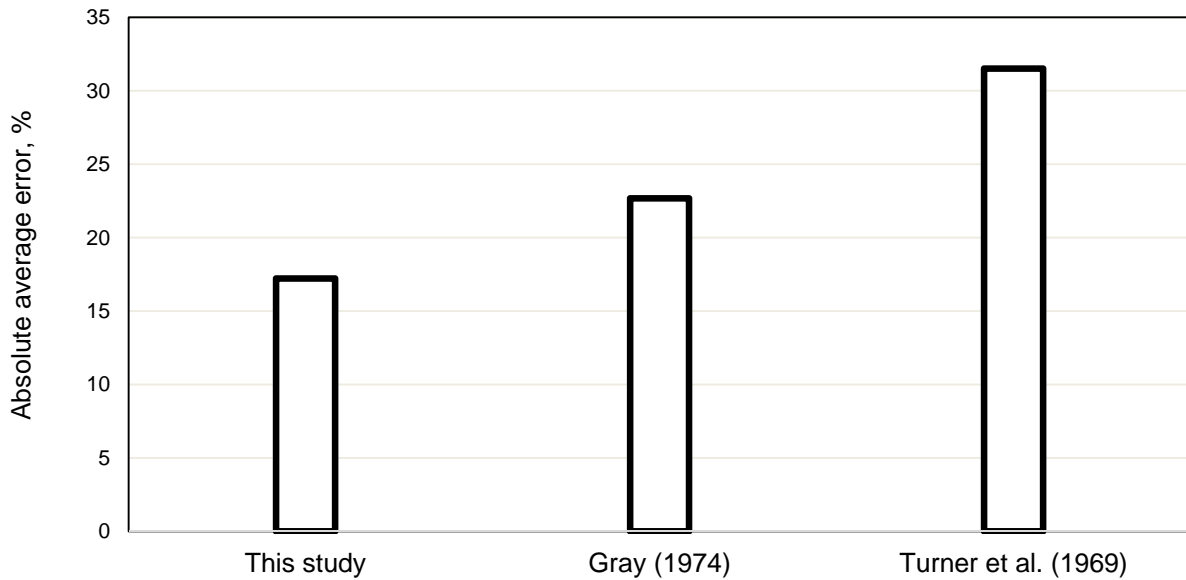
The model validation results for all ten wells are shown in Figure 4.11. From these results, it is possible to conclude that the model proposed in this study using the TPR correlation proposed in this study has an overall better performance than the flow correlation of Gray (1974) and Turner critical flow rate.

It is important to point out the fact that the absolute average error for the proposed model using the TPR correlation proposed in this study stayed within the range of +17%, which is within the range of the accuracy of the flow measurements ( $\pm 20\%$ ) for the field data published by Veeken et al. (2010). When using Gray (1974) correlation for the TPR curve, the average error is slightly greater than 20%, which means that the concept of IPR tangent to the TPR curve still works with a reasonable accuracy when using Gray correlation. However, the TPR correlation proposed in this study has shown to be more accurate than Gray's for low and high gas rates. Larger deviations when using Gray (1974) correlation for low-pressure low-gas rates are also observed on the studies of Waltrich et al. (2015b) and in this study (shown in Section 4.1) using laboratory and field data.





(a)



(b)

Figure 4.11 – (a) Relative error, and (b) absolute average error for the comparison between field data published by Veeken et al. (2010) for the predicted minimum flow rate for liquid loading initiation. These results show the prediction for the field data using the concept of IPR tangent to the TPR proposed, using TPR model proposed in this study and Gray (1974). Turner et al. (1969) critical flow rate is also compared to the same field data set. The angle ( $\theta$ ) above the x-axis in figure (a) indicates the inclination of the well.

The droplet model of Turner et al. (1969) resulted in an average error of approximately 32%, which is significantly larger than the accuracy of the flow measurement of  $\pm 20\%$ . It is also important to mention that for some wells in the data set of Veeken et al. (2010), Turner et al. (1969) critical flow rate is lower than the minimum flow for the tangent point of intersection between IPR and TPR.

If one assumes that the IPR and TPR curves are good physical representations of the fluid flow behavior in the reservoir and wellbore (which is a widely accepted assumption), the minimum flow rate predicted by the Turner (1969) correlation would be physically impossible, as the minimum flow rate possible for a well is at the tangent between the IPR and TPR curves. In other words, in order for the reservoir to deliver the fluids to the surface through the wellbore, the IPR curve needs to intersect the TPR curve. At a gas flow rate lower than the tangent between the IPR and TPR curves, the IPR and TPR can no longer cross each other, so flow from reservoir to the surface through the wellbore is no longer possible.

Two other important features for the field data of Veeken et al. (2010), which makes the validation in this study relevant are the wide range of productive index ( $J$ ) and wellbore diameter included in this database. As concluded by Riza et al. (2015) after a parametric study, productivity index and wellbore diameter are the dominate parameters in the determination of minimum flow rate for liquid loading initiation. Also, the same dataset features a wide range of wellhead pressures, minimum flow rates, and well inclinations. Belfroid et al. (2008) suggested that the Turner critical velocity should be modified to work appropriately on wells with inclinations other than vertical. In fact, as it is shown in Figure 4.11a, Turner's criterion have higher relative errors for larger well inclinations, while the model in this study shows only an

average error around 20% for such wells, which is still within the data measurement uncertainty of ( $\pm 20\%$ ).

#### **4.2.1 Testing the Concept of Minimum Pressure Point and Nodal Analysis (Lea et al., 2003) with Field Data of Veeken et al. (2010)**

The approach of using the IPR tangent to the TPR curve is also compared to the concept of minimum pressure as previously described by Lea et al. (2003) (see Section 3.2). For each well, the TPR had already been calculated using the model proposed in this study and Gray (1974) correlation. Thus, to estimate the liquid loading initiation using the concept of minimum pressure, only one additional step to determine the lowest pressure value for each TPR is needed. After these values are determined, the results for all the 10 wells are presented in Figure 4.12.

The results for the droplet model of Turner et al. (1969) are also included. From Figure 4.12a, it is possible to conclude that the error using the model for TPR proposed in this study provides better results than the Gray (1974) correlation.

Figure 4.12b compares the concept of minimum pressure and the method of using IPR tangent to the TPR curve. From this figure, it is clear to see that the concept of the IPR tangent to the TPR curve provide better results than the minimum pressure method. When using the model proposed in this study for the TPR, and the concept of IPR tangent to the TPR to predict liquid loading initiation, the average error resulted in only 17%, while the average error was around 23% when using same concept but with the Gray (1974) correlation. The critical flow rate criterion of Turner shows a superior prediction when compared to the minimum pressure concept of Lea et al. (2003), but the Turner criterion has significantly larger errors when using the method of IPR tangent to TPR, particularly when using the TPR based on the model proposed in this study for churn and annular flow regimes.

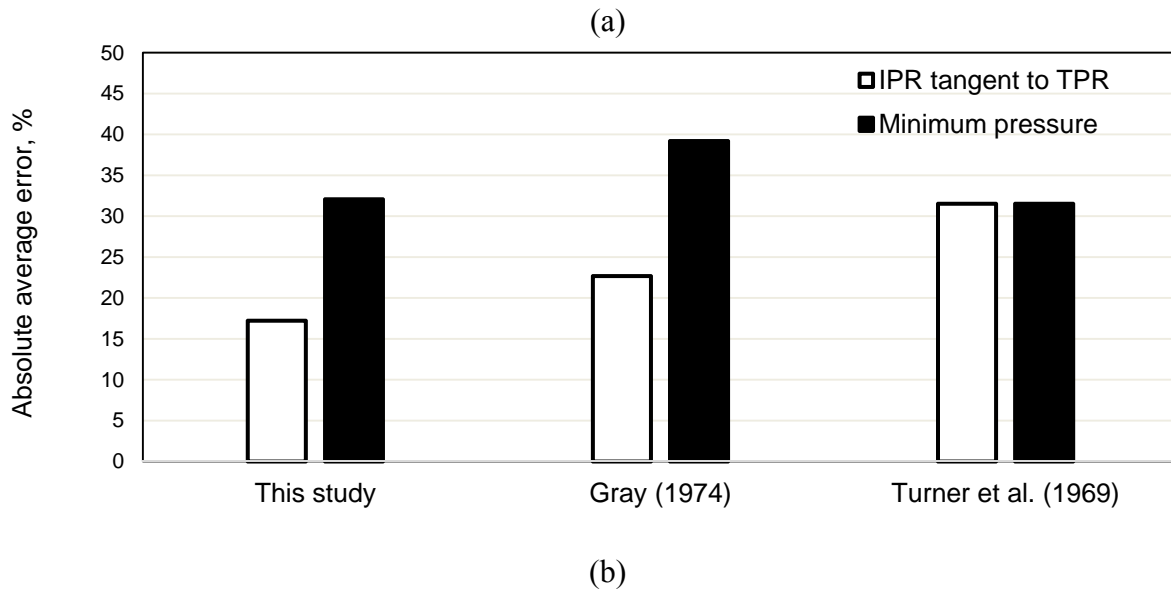
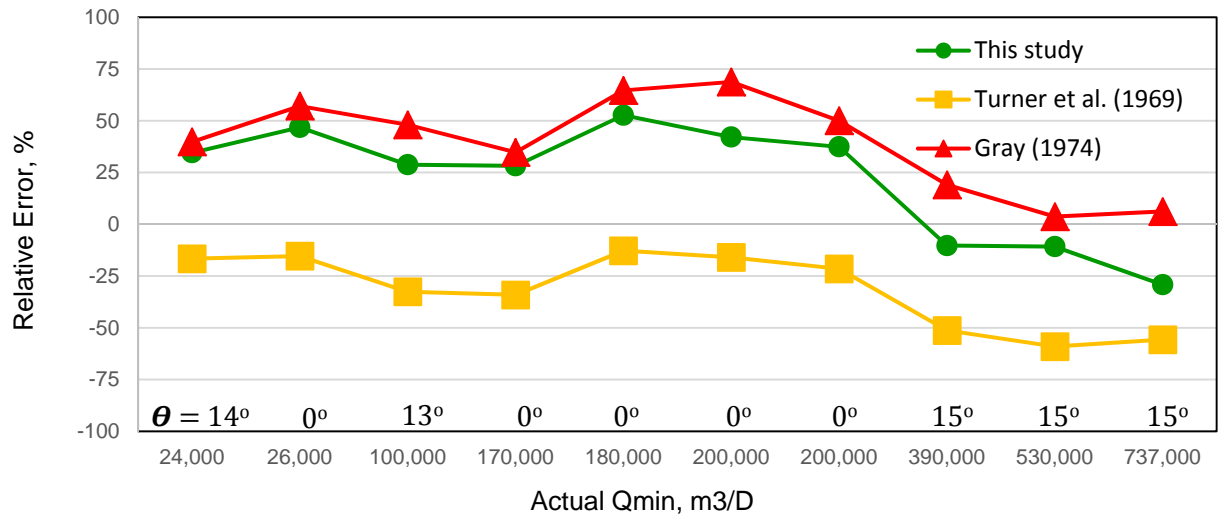


Figure 4.12 – (a) Relative error and (b) absolute average error for the comparison between field data published by Veeken et al. (2010) for the predicted minimum flow rate for liquid loading initiation when using the concept of minimum pressure of Lea et al. (2003) with the TPR model proposed in this study and Gray (1974). Figure 4.12b also includes the results previously presented in Figure 4.11b. The results for Turner et al. (1969) critical flow rate are also compared. The angle ( $\theta$ ) above the x-axis in figure (a) indicates the inclination of the well.

#### 4.2.2 Explaining Liquid Loading Field Symptoms Using the Proposed Model

This section shows how to use the model proposed in this study for prediction of liquid loading initiation to describe the field symptoms observed for a gas well under liquid loading conditions.

Some gas well operators identify these symptoms using field production data to diagnose when their wells are suffering from liquid loading. However, the identification of such symptoms in the field is highly subjective. In addition to that, not all of these symptoms are present at the same time. The following list presents the major field symptoms associated with liquid accumulation in the wellbore (Lea and Nickens, 2004):

- Symptom 1: Increase of liquid content in the wellbore
- Symptom 2: Sudden drop in gas production
- Symptom 3: Significant change in pressure gradient along the wellbore
- Symptom 4: Liquid slugs arriving in the surface
- Symptom 5: Pressure spikes in wellbore flowing pressure

To show how the proposed model can be used to describe the field symptoms associated to liquid loading, the model is implemented using a reservoir with initial-gas-in-place of  $1.47 \times 10^9 \text{ Sm}^3$  ( $50 \times 10^9 \text{ scf}$ ), a vertical wellbore of 0.1016 m (4 in) internal diameter, and a wellbore depth of 3,350 m (10,990 ft). The wellhead pressure and temperature are considered as 17 bar (250 psig) and 23.9 °C (75 ° F), respectively. A productivity index of  $0.005 \times 10^3 \text{ Sm}^3/\text{D}/\text{bar}^2$  ( $0.0009 \text{ Mscf}/\text{D}/\text{psi}^2$ ) is assumed.

Figure 4.13 shows the results for the liquid holdup as a function of time for this simulated case, using the TPR model proposed in this study (Section 3.1).

As described by Symptom 1 in the list above, gas well operators observe an increase in liquid content in the wellbore as the wellbore reaches liquid loading conditions. As a consequence of the exponential increase in liquid holdup, bottomhole pressure also increases, which leads to an exponential and sudden decrease in gas production rate, as shown in Figure 4.14 (Symptom 2). In fact, the study of Waltrich et al. (2015a) used video recordings in a long

(42-m high) and transparent vertical tube to show that a sudden change in gas flow rate can lead to liquid falling to the bottom of the tube.

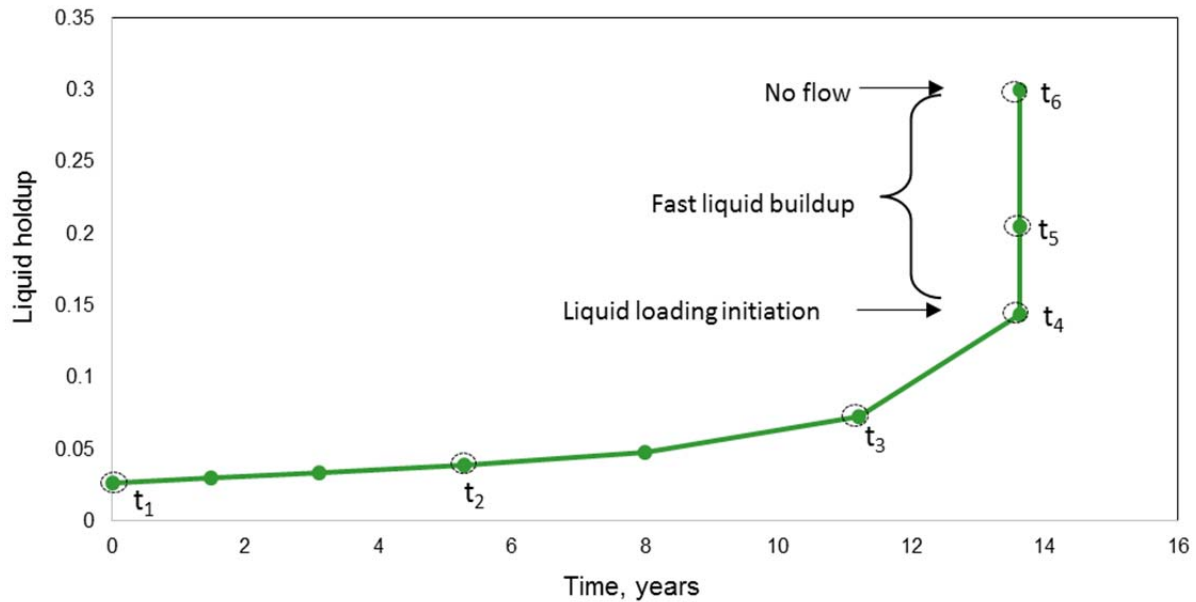


Figure 4.13 – Simulated results shows the increase on wellbore liquid holdup over time using the proposed model with correlation for TPR proposed in this study. This increase in liquid content in the wellbore is often correlated in the field to liquid loading symptoms.

The latter authors also show that after a sudden change in gas flow rate, there is a significant change in pressure gradient along the wellbore (Symptom 3), as a consequence of larger liquid content in the bottom of the tube. However, the steady-state pressure gradient for the new lower gas rate is slowly re-established as liquid flow upwards, as long as liquid and gas injection rates are continued. The experiments of Waltrich et al. (2015a) also show that after this sudden change in gas rate, there is a significant increase in the pressure oscillation along the tube (Symptom 5), and it is possible to observe a high amount of liquid content flowing upward in the tubing (Symptom 4). Furthermore, the experiments of Waltrich et al. (2015a) showed through video recordings and simulation results that the liquid droplets are flowing upwards, for gas velocities lower than the critical criterion of Turner et al. (1969). Thus, this study brings more

evidences that the droplet model of Turner may not be appropriate to describe the basic physics of the flow for liquid loading initiation. The comparison with field data presented in Figure 4.11b also shows the limitations of Turner critical velocity concept.

Figure 4.14 shows the results for the gas production rate as a function of time for this simulated case. This figure also compares how the use of different flow correlations for the TPR predicts the time to reach liquid loading initiation.

The time difference between the model to predict liquid loading initiation using the model proposed in this study for the TPR and Gray (1974) correlation is more than 4 years. An important observation from the results in Figure 4.14 is the significant impact that different wellbore flow models can have on the prediction of the “death” of the well.

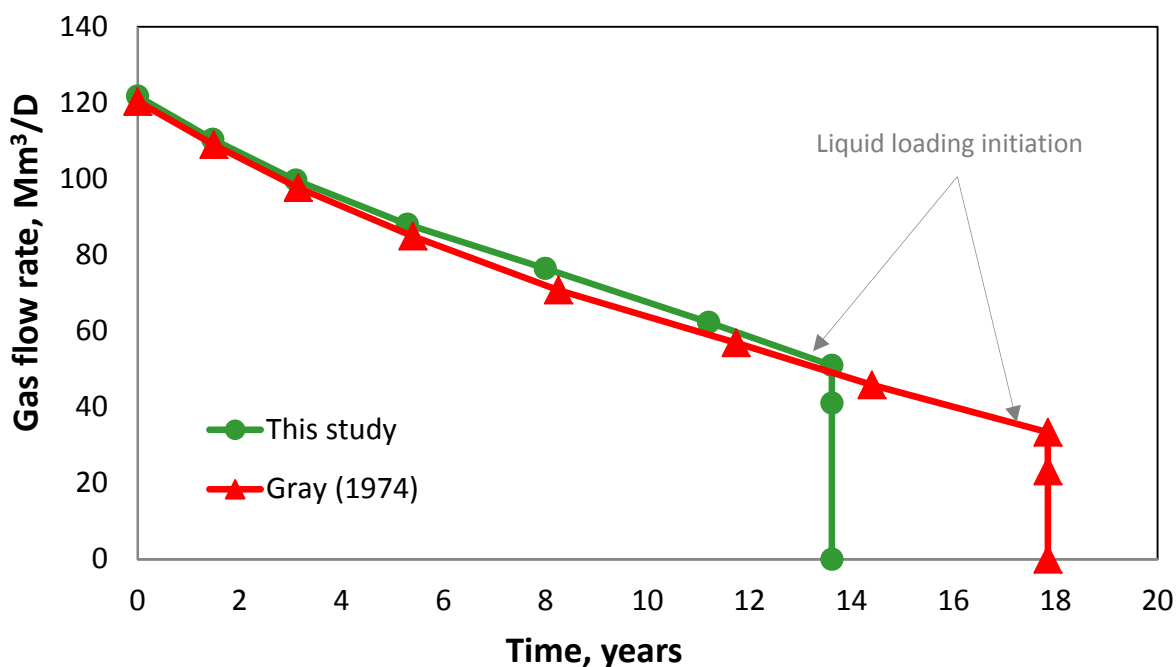


Figure 4.14 – Simulated results for decline in production rate over time using the correlation for the TPR proposed in this study, and Gray (1974) correlation. The sharp and sudden change gas rate indicates the liquid loading initiation. The explanation for the large divergence between the model proposed in this study and other popular flow correlation is a consequence of the difference in predicted bottomhole pressure for low gas rates as shown in Figure 4.10.

Waltrich et al (2015b) have shown that widely-used wellbore flow correlations (such as Gray, 1974) have a poor prediction for low-liquid, low-gas and low-pressure two-phase flows in long vertical tubes. The use of model proposed in this study for flows under churn and annular conditions (TPR model) has shown to be more accurate to predict liquid loading initiation (see Figure 4.11) for a wide range of conditions. The model proposed in this study has shown that this TPR model has a good prediction for low- and high-liquid, low- and high-gas and low- and high-pressure two-phase flows in short and long vertical and near-vertical tubes with small and large diameters (see model validation in Section 4.1).

As shown in Figure 4.10, both this study and Gray (1974) models have similar results for the bottomhole pressure until close to the minimum point. However, for gas flow rates lower than the minimum point, there is a significant discrepancy between these models. The main reason for this difference is the inclusion of a more robust churn flow model in this study. Gray (1974) correlation was not originally developed for low-pressure low-gas rate conditions, and it may not give good predictions for these conditions, as stated previously in the study of Oudeman (1990). The model proposed in this thesis was developed and validated for a wide range of pipe diameters, pressure, and flow rates, including low-pressure low-gas low-liquid rate conditions.

The model proposed in this study assumes that the reservoir does not have enough pressure at the bottom of the wellbore to sustain steady-state flow for gas flow rates lower than  $Q_{min}$ . Once the pressure in the reservoir is not enough, gas production rate starts to decrease suddenly, which consequently leads to liquid falling back to the bottom of the wellbore. The results in Figure 4.14 show only one cycle for a well under liquid loading conditions. A new cycle would start as the liquid is drained back to the formation as suggested by Dousi et al. (2006). Once the wellbore liquid holdup drops below the amount of liquid at liquid loading



initiation, the gas production would re-start (assuming a constant wellhead pressure). The metastable flow could be also modeled here as proposed by Dousi et al. (2006), but the focus on this thesis is to show the liquid loading initiation using nodal analysis and abandonment pressure concept rather than simulating metastable flows.

Figure 4.15 shows the results for the simulated case (using TPR proposed in this study – Section 3.1) using a schematic representation in terms of production gas rate,  $Q_g$  (in Mscf/D), liquid holdup,  $H_l$ , and flow regimes at the different times in the life of the well.

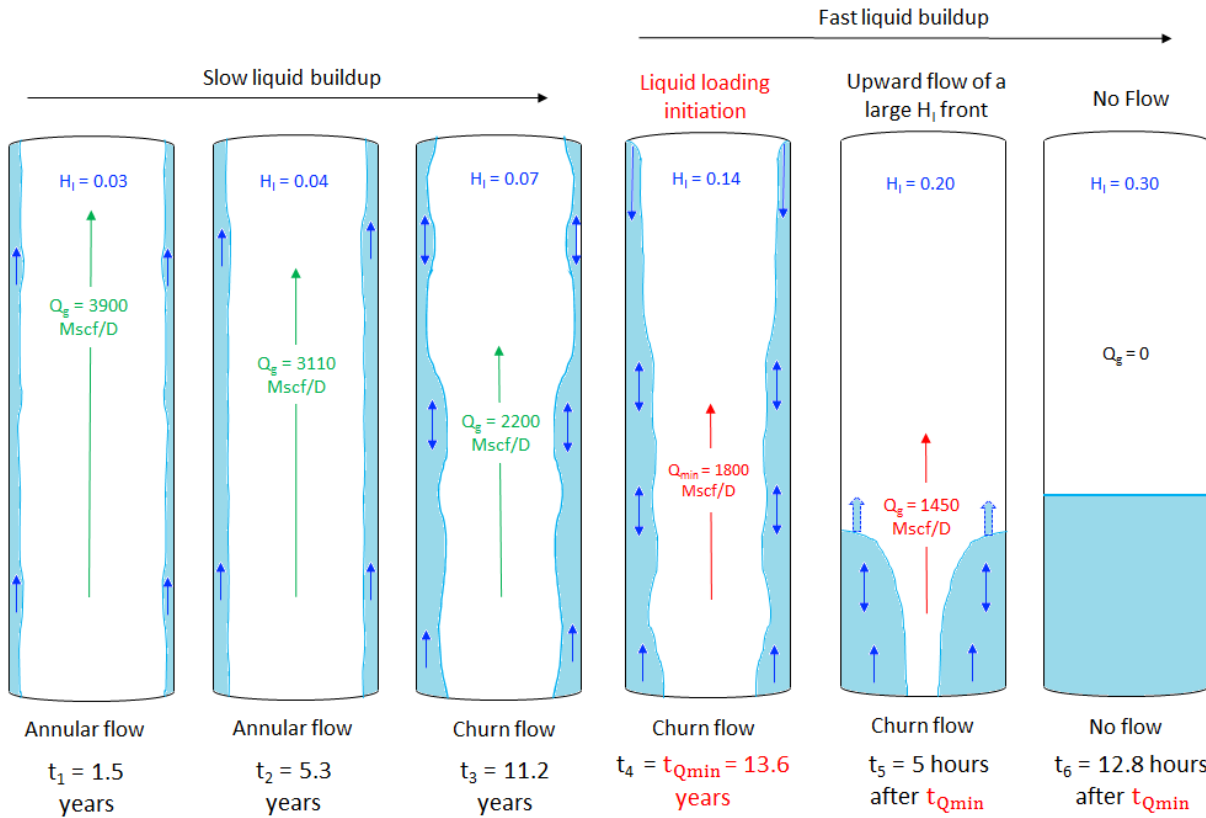


Figure 4.15 – Schematic representation of the change in wellbore liquid holdup, for different times for the simulated case.

This schematic representation presents how the gas-liquid flow behaves inside the wellbore from time  $t_1$  to  $t_6$ . The arrows represent the flowing direction of the fluids. At times  $t_1$  and  $t_2$  both liquid and gas phases flow in the upward direction. During this period of time, the

fluids are flowing with an annular flow regime (upward thin wall liquid film and a gas core with a few entrained droplets). Reservoir pressure keeps decreasing with time, and so, gas production rate also decreases. As a consequence, the liquid volume fraction (liquid holdup) increases with time, considering a constant liquid inflow from the reservoir. Thus, at time  $t_3$  the liquid film becomes thicker and starts flowing in both upwards and downwards direction, even though the net liquid film direction is upward. At this time, the fluids are flowing in churn flow regime (thick and oscillatory wall liquid film, with large lumps of liquid flowing upward in the gas core). Then, after 13.6 years of production ( $t_4$ ), the reservoir pressure is no longer enough to lift the fluids up to the surface through this wellbore. The wellbore is said to be under liquid loading conditions from this time. After time  $t_4$ , liquid starts to rapidly fall down to the bottom of the well. Thus, liquid holdup and bottomhole pressure increases exponentially (note that the difference in time  $t_4$  and  $t_5$  is only 5 hours) until gas production ceases completely at time  $t_6$ , only 12.8 hours after well starts suffering from liquid loading.

## 5. Conclusions and Recommendations for Future Work <sup>1, 2</sup>

This chapter presents the conclusions of this study, and it is divided into two main sections, as in chapters 2 to 4. The first section describes the conclusions for the development and validation results for two-phase flow in churn and annular flow regimes for vertical and near-vertical pipes. The second section presents the main conclusions for the application of the concept of liquid loading initiation based on the point that the IPR curve is tangent to the TPR curve. Both sections recommend ideas for future work in continuation of this study.

### 5.1 Conclusions on the Churn and Annular Flow Modeling

This study presented a new model for churn-annular vertical and near-vertical two-phase flows for small and large diameters pipes. This model modified the empirical correlations previously proposed by other investigators for the interfacial friction factor for churn and annular flow regimes. This model does not require the use of empirical correlations for the entrainment fraction for annular flow regime, which is necessary for most of the mechanistic models for this regime. The model is validated and compared to laboratory and field data. From the comparison with the data set collected, the following conclusions can be drawn from this study:

- The performance of the model proposed in this study and other widely used flow correlations were compared with laboratory data, for pipe diameters ranging from 0.032 m (1.252 in) to 0.2794 m (11 in).
- The model proposed in this study showed a reasonable agreement to experimental data

---

<sup>1</sup>Section 5.1 of this chapter previously appeared as E. Pagan, W. C. Williams, S. Kam, P. J. Waltrich, Modeling Vertical Flow in Churn and Annular Flow Regimes in Small- and Large-Diameter Pipes, Paper Presented and Published at BHR Group's 10th North American Conference on Multiphase Technology 8-10th June 2016. It is reprinted by permission of Copyright © 2016 BHR Group. See Appendix for more details.

<sup>2</sup>Section 5.2 of this chapter previously appeared as Erika V. Pagan, Wesley Williams, and Paulo J. Waltrich, A Simplified Transient Model to Predict Liquid Loading in Gas Wells, Paper SPE-180403-MS presented at the SPE Western Regional Meeting held in Anchorage, Alaska, USA, 23-26 May 2016. It is reprinted by permission of Copyright 2016, Society of Petroleum Engineers Inc. Copyright 2016, SPE. Reproduced with permission of SPE. Further reproduction prohibited without permission. See Appendix for more details.

(for pressure gradient and liquid holdup), for the entire range of superficial gas and liquid velocities tested. The absolute average error on the prediction of the experimental pressure is 36% for the model proposed in this study. Other flow models widely used in the oil and gas industry are also compared to the same experimental pressure gradient database, which all showed absolute average errors larger than the model proposed in this study.

- The inclusion of a separate model for churn flow regime has shown to provide better results in terms of pressure gradient for both small and large pipe diameters. Most of the other models evaluated in this study, which exhibited larger errors, showed a poor performance likely as consequence of simulating churn flow with either slug flow or annular flow regimes. Thus, it is concluded that the churn flow regime should be considered as separate flow regime to improve predictions of the pressure gradient in vertical and near-vertical two-phase flows for small and large pipe diameters.

The model proposed in this study is also deployed to predict field data for pressure profile in the wellbore (field data of Fancher and Brown, 1963) and in terms of wellbore bottomhole pressure with well inclinations up to 8.2 degrees off-vertical (data of Reinicke et al., 1987). Field data included wellbore diameters ranging from 0.05 (2 in) to 0.124 m (4.96 in). The prediction for the pressures along the well (Fancher and Brown, 1963) resulted in an average error of only 5 %, for 12 wells tested with diameter of around 0.05 m (2 in). Furthermore, the predictions for the bottomhole pressure using the model proposed in this study for wellbores with diameter around 0.101m (3.976 in) stayed within the deviation range of  $\pm 20\%$ , for 24 wells simulated. The average error including all 24 wells is only 6%.

For future work, the following recommendations are proposed on the modeling for churn and annular flow regimes:

- The development and inclusion of a model for bubble and slug flow to the model proposed in this study, in order for the model to include all the flow regimes for vertical and near-vertical flows.
- The development and inclusion of a model to estimate flow behavior in horizontal and near-horizontal wells.
- Study of flow regime transitions for all well inclinations.

## **5.2 Conclusions on Liquid Loading Modeling**

This study also presented a model to predict liquid loading initiation, by using the concept of the tangent of the IPR and TPR curves in a nodal analysis (see Figure 3.2), and its transient effects, which can be calculated by using Equations (3.23) to (3.25) and are described in Section 4.2.2.

The proposed model was validated with field data for a wide range of conditions. Based on the validation and simulation results, the following conclusions can be drawn from this study:

- The proposed model showed an overall better performance than conventional techniques for predicting liquid loading initiation when compared to field data for ten wells, for a wide range of conditions. The proposed approach of using the IPR tangent to the TPR curves showed an overall better performance when compared to the widely accepted critical velocity criterion of Turner et al. (1969). The average absolute error for predicting liquid loading initiation is 17% for the approach proposed in this study, while for the Turner critical velocity criterion the average absolute error is 32%.

- The major symptoms observed in the field for gas wells under liquid loading conditions are described through simulated results using the proposed model. These results also show that the “early death” of gas wells could be associated to the poor prediction of widely used tubing performance relationship correlations.
- The model proposed in this study accurately predicted liquid loading initiation assuming that the reservoir cannot provide enough bottomhole pressure to sustain steady-state flow in the wellbore for gas flow rates lower than the critical gas flow rate. Once gas flow rate reaches the minimum flow for liquid loading initiation, gas production rate starts to decrease suddenly, which consequently leads to liquid falling back to the bottom of the wellbore.

Although the overall performance for a wellbore flow correlation is important, the trend of bottomhole pressure with the change of gas flow rate plays a major role on the prediction of liquid loading initiation. The validation results showed that the tangent of the wellbore flow model (TPR) with the reservoir inflow model (IPR) provide a good approach to predict liquid loading initiation when compared to field data. The TPR model of this study (Section 3.1) and the Gray (1974) correlation are compared. Both models show similar results for gas flow rate above the minimum pressure point. However, for gas flow rates below the minimum pressure point, significant differences are observed, which can considerably impact the prediction of liquid loading initiation.

For future work, the following recommendations are proposed on the modeling for liquid loading initiation:

- Further validation of the concept of tangent in the nodal analysis using different wells from several different geographical locations.

- Inclusion of a model to estimate production (metastable flow) when a new cycle starts after liquid loading initiation. This new cycle happens as the liquid accumulated in the bottom of the well (due liquid loading phenomenon) is drained back to the formation as suggested by Dousi et al. (2006).
- Validate the concept of the new TPR proposed in Figure 3.2 from time  $t_4$  to time  $t_6$  with field or experimental data, which states that the bottomhole pressure values is the same as indicated by the IPR curve for gas rates lower than  $Q_{min}$ .

## References

- Ali, S. F. 2009. Two Phase Flow in Large Diameter Vertical Riser. PhD thesis, Cranfield University, Bedfordshire.
- Alves, M. V. C. 2014. Modelagem Numerica do Escoamento Transient Churn-Annular em Tubulacoes Verticais e sua Aplicacao na Simulacao de Carga de Liquido em Pocos de Gas. PhD thesis, Universidade Federal de Santa Catarina, Florianopolis, Santa Catarina (April 2014).
- Ansari, A. M., Sylvester, N. D., Sarica, C. Shoham, O., and Brill, J. P. 1994. A Comprehensive Mechanistic Model for Upward Two-Phase Flow in Wellbores. *SPE Production and Facilities*, **9** (02): 143-152. SPE-20630-PA. <http://dx.doi.org/10.2118/20630-PA>.
- Barbosa, J. R., Govan, A.H., and Hewitt, G. F. 2001. Visualisation and modelling studies of churn flow in a vertical pipe. *Int. J. Multiphase Flow* **27**: 2105–2127.
- Belfroid, S. P. C., Schiferli, W., Alberts, G. J. N., Veeken, C. A. M., and Biezen, E. 2008. Prediction Onset and Dynamic Behaviour of Liquid Loading Gas Wells. Paper SPE-115567-MS presented at the SPE Annual Technical Conference and Exhibition, 21-24 September, Denver, USA. <http://dx.doi.org/10.2118/115567-MS>.
- Bendiksen, K.H., Maines, D., Moe, R., and Nuland, S. 1991. The Dynamic Two-Fluid Model Olga: Theory and Application. *SPE Production Engineering* **6** (2). <http://dx.doi.org/10.2118/19451-PA>.
- Bharathan, D., Richter, H. J., and Wallis, G. B. 1978. Air-water counter-current annular flow in vertical tubes. Report EPBI-NP-786.
- Bharathan, D., and Wallis, G.B. 1983. Air-water counter-current annular flow. *Int. J. Multiphase Flow*, **9** (4): 349-366.
- Brauner, N., and Barnea, D. 1986. Slug/Churn transition in upward gas-liquid flow. *Chemical Engineering Science*. **41**, 159–163.
- Brill, J. P., and Mukherjee, H. K. 1999. *Multiphase Flow in Wells*, first printing. Richardson, Texas: Society of Petroleum Engineers Incorporated (Reprint).
- Coleman, S. B., Hartley, B. C., McCurdy, M. G., and Norris III, L. H. 1991. A New Look at Predicting Gas-Well Load-Up. *J Pet Tech* **43** (3): 329-333. <http://dx.doi.org/10.2118/20280-PA>.
- Chupin, G., Hu, B., Haugset, T., Sagen, J., and Claudel, M. 2007. Integrated



Wellbore/Reservoir Model Predicts Flow Transients in Liquid-Loaded Gas Wells. Paper SPE-110461-MS presented at the SPE Annual Technical Conference and Exhibition, Anaheim, California, USA, 11–14 November.. <http://dx.doi.org/10.2118/110461-MS>.

Beggs, D. H., and Brill, J. P., 1973. A study of two-phase flow in inclined pipes. *J. Petroleum Technology*. **25** (05), 607-617. SPE-4007-PA. <http://dx.doi.org/10.2118/4007-PA>.

Bureau of Ocean Energy Management, Regulation, and Enforcement. 2010. NTL No. 2010-N06, Information Requirements for Exploration Plans, Development and Production Plans, and Development Operations Coordination Documents on the OCS, Washington, DC. US Department of the Interior. <http://www.boem.gov/Regulations/Notices-To-Lessees/2010/10-n06.aspx>.

Dousi, N., Veeken, C. A. M., and Currie, P. K. 2006. Numerical and Analytical Modeling of the Gas-Well Liquid Loading Process. *SPE Prod Opns*. **21** (4): 475-482. <http://dx.doi.org/10.2118/95282-PA>.

Dukler, A. E. and Taitel, Y. 1986. Flow Pattern Transition in Gas-Liquid Systems: Measurement and Modeling. *Multiphase Science and Technology* **2** (1-4): 1-94.

Duns Jr., H., and Ros, N. C. J., 1963. Vertical flow of gas and liquid mixtures in wells. In 6<sup>th</sup> World Petroleum Congress, Frankfurt am Main, Germany, 19-26 June.

Economides, M. J., Hill, A. D., Ehlig-Economides, C. E., and Zhu, D. 2013 *Petroleum Production Systems*. Prentice Hall, Englewood Cliffs, New Jersey.

Fancher Jr., G. H., and Brown, K. E. 1963. Prediction of Pressure Gradients for Multiphase Flow in Tubing. *SPE Journal*, **3** (01): 59-69.

Govan, A. H., Hewitt, G. F., Richter, H. J., and Scott, A. 1991. Flooding and Churn Flow in Vertical Pipes. *International Journal of Multiphase Flow* **17** (1): 27-44.

Gray, H. E. 1974. Vertical Flow Correlation in Gas Wells. *User's Manual for API 148 Subsurface Controlled Safety Valve Sizing Computer Program*, Appendix B.

Hagedorn, A. R., and Brown, K. E. 1965. Experimental study of pressure gradients occurring during continuous two-phase flow in small-diameter vertical conduits. *J. Petroleum Technology* **17** (04), 475-484. SPE-940-PA. <http://dx.doi.org/10.2118/940-PA>.

Hewitt, G. F., and Hall-Taylor, N. S. 1970. *Annular Two-Phase Flow*, first edition. Oxford, New York: Pergamon Press.

Hewitt, G. F., Martin, C.J., and Wilkes, N. S. 1985. Experimental and modelling studies of annular flow in the region between flow reversal and the pressure drop minimum. *PCH, Physico Chemical Hydrodynamics*. **6** (1-2): 69-86.

Hewitt, G. F., and Wallis, G. B. 1963. Flooding and associated phenomena in falling film in a vertical tube. Proceedings of Multi-Phase Flow Symposium, Philadelphia, PA, 17–22 November: 62–74.

Hewitt, G. F. 1982. *Handbook of Multiphase Flow Systems*. New York: Hemisphere Publishing Corporation.

Hewitt, G. F. 2012. Churn and Wispy Annular Flow Regimes in Vertical Gas–Liquid Flows. *Energy Fuels*, **26** (8): 4067-4077.

Hu, B., Veeken, K., Yusuf, R., and Holmås, H. 2010. Use of Wellbore-Reservoir Coupled Dynamic Simulation to Evaluate the Cycling Capability of Liquid-Loaded Gas Wells. Paper SPE-134948-MS presented at the SPE Annual Technical Conference and Exhibition, 19–22 September, Florence, Italy. <http://dx.doi.org/10.2118/134948-MS>.

Jayanti, S., and Brauner, N. 1994. Churn Flow. *Multiphase Science and Technology* **8**: 471-522.

Jayanti, S. and Hewitt, G. F. 1992. Prediction of the Slug-to-Churn Flow Transition in Vertical Two-Phase Flow. *Int. J. Multiphase Flow* **18** (6): 847-860.

Kaya, A. S., Sarica, C., and Brill, J. P. 2001. Mechanistic Modeling of Two-Phase Flow in Deviated Wells. Society of Petroleum Engineers. doi:10.2118/72998-PA.

Lea, J. F., Nickens, H. V., and Wells, M.R. 2003. *Gas Well Deliquification*: Elsevier. Original edition. ISBN 978-0-7506-8280-0.

Lea, J. F., and Nickens, H. V. 2004. Solving Gas-Well Liquid-Loading Problems. *J Pet Tech* **56** (4): 30-36. <http://dx.doi.org/10.2118/72092-JPT>.

Li, X. 2013. A Combined Bottom-hole Pressure Calculation Procedure using Multiphase Correlations and Artificial Neural Networks Models. MS thesis, Colorado School of Mines, Colorado.

Limpasurat, A., Valko, P. P., and Falcone, G. 2015. A New Concept of Wellbore-Boundary Condition for Modeling Liquid Loading in Gas Wells. Paper SPE-166199-PA presented at the SPE Annual Technical Conference and Exhibition, 30 September – 2 October, New Orleans, USA. <http://dx.doi.org/10.2118/166199-PA>.

- OLGA Dynamic Multiphase Flow Simulator. 2000. Schlumberger.
- Omebere-Yari, N. K., and Azzopardi, B. J. 2007. Two-Phase Flow Patterns in Large Diameter Vertical Pipes at High Pressures. *AIChE J.* **53** (10): 2493-2504.
- Oudeman, P. 1990. Improved Prediction of Wet-Gas-Well Performance. *SPE Prod Eng* **5** (3): 212-216; *Trans.*, AIME, 289. SPE-19103-PA. <http://dx.doi.org/10.2118/19103-PA>.
- Owen, D. G. 1986. An Experimental and Theoretical Analysis of Equilibrium Annular Flow. PhD thesis, University of Birmingham, Birmingham, UK.
- PIPESIM Multiphase Flow Simulator. 2013. Schlumberger.
- Pushkina, O. L., and Sorokin, Y. L. 1969. Breakdown of Liquid Film Motion in Vertical Tubes. *Heat Transfer Soviet Research.* **1** (5): 56-64.
- Reinicke, K. M., Remer, R. J., and Hueni, G. 1987. Comparison of Measured and Predicted Pressure Drops in Tubing for High-Water-Cut Gas Wells. *SPE Prod Eng* **2** (3): 165-77; *Trans.*, AIME, 283. SPE-13279-PA. <http://dx.doi.org/10.2118/13279-PA>.
- Riza, M. F., Hasan, A. R., and Kabir, C. S. 2014. A Pragmatic Approach to Understanding Liquid Loading in Gas Wells. Paper SPE-170583-MS presented at SPE Annual Technical Conference and Exhibition, 27-29 October, Amsterdam, The Netherlands. <http://dx.doi.org/10.2118/170583-MS>.
- Rygg, O. B., and Gilhuus, T. 1990. Use of a Dynamic Two-Phase Pipe Flow Simulator in Blowout Kill Planning. SPE Annual Technical Conference and Exhibition, 23-26 September, New Orleans. <http://dx.doi.org/10.2118/20433-MS>.
- Shoham, O. 2006. *Mechanistic modeling of gas-liquid two-phase flow in pipes*. Richardson, TX: Society of Petroleum Engineers (Reprint).
- Skopich, A., Pereyra, E. Sarica, C., and Kelkar, M. 2015. Pipe Diameter Effect on Liquid Loading in Vertical Gas Wells. *SPE Prod Opns.* Paper SPE-164477-PA presented at the SPE Production and Operations Symposium, 23-26 May, Oklahoma, USA. <http://dx.doi.org/10.2118/164477-PA>.
- SPE. 2015. Calculation of Worst-Case Discharge (WCD). SPE Technical Report. Society of Petroleum Engineers. Richardson.
- Taitel, Y., Barnea, D. and Dukler, A. E. 1980. Modeling Flow Pattern Transitions for Steady Upward Gas-Liquid Flow in Vertical Tubes. *AIChE J.* **26** (3): 345-354.

Takacs, G. 2001. Considerations on the Selection of an Optimum Vertical Multiphase Pressure Drop Prediction Model for Oil Wells. SPE/ICoTA Coiled Tubing Roundtable, 7-8 March, Houston, Texas. <http://dx.doi.org/10.2118/68361-MS>.

Tengesdal, J. O., Kaya, A. S., and Sarica, C. 1999. Flow-Pattern Transition and Hydrodynamic Modeling of Churn Flow. SPEJ, 342.

Turner, R. G., Hubbard, M. G., and Dukler, A. E. 1969. Analysis and Prediction of Minimum Flow Rate for the Continuous Removal of Liquids from Gas Wells. *J Pet Technol* **21** (11): 1475-1482. SPE-2198-PA. <http://dx.doi.org/10.2118/2198-PA>.

Van der Meulen, G. P. 2012. Churn-Annular Gas-Liquid Flows in Large Diameter Vertical Pipes. PhD thesis, University of Nottingham, Nottinghamshire.

Veeken, K., Hu, B., and Schiferli, W. 2010. Gas-Well Liquid-Loading-Field-Data Analysis and Multiphase-Flow Modeling. *SPE Prod Opns.* **25** (3): 275-284. <http://dx.doi.org/10.2118/123657-PA>.

Wallis, G. 1969. *One Dimensional Two-Phase Flow*. New York: McGraw-Hill.

Waltrich, P. J. 2012. Onset and Subsequent Transient Phenomena of Liquid Loading in Gas Wells: Experimental Investigation Using a Large Scale Flow Loop. PhD thesis, Texas A&M University, Texas.

Waltrich, P. J., Falcone, G., and Barbosa Jr, J.R. 2013. Axial Development of Annular, Churn and Slug Flows in a Long Vertical Tube. *Int J Multiphase Flow* **57**: 38–48. <http://dx.doi.org/10.1016/j.ijmultiphaseflow.2013.06.008>.

Waltrich, P. J., Falcone, G., and Barbosa Jr., J. R. 2015a, Liquid Transport During Gas Flow Transients Applied to Liquid Loading in Long Vertical Pipes. *Experimental Thermal and Fluid Science*, Elsevier. <http://dx.doi.org/10.1016/j.expthermflusci.2015.07.004>.

Waltrich, P. J., Posada, C., Martinez, J., Falcone, G., and Barbosa Jr., J. R. 2015b. Experimental Investigation on the Prediction of Liquid Loading Initiation in Gas Wells Using a Long Vertical Tube. *Journal of Natural Gas Science and Engineering*, Elsevier. <http://dx.doi.org/10.1016/j.jngse.2015.06.023>.

van 't Westende, J. M. C., Kemp, H. K., Belt, R. J., Portela, L. M., Mudde, R. F., and Oliemans, R. V. A. 2007. On the Role of Droplets in Cocurrent Annular and Churn-Annular Pipe Flow. *International Journal of Multiphase Flow* **33** (6): 595-615. doi:10.1016/j.ijmultiphaseflow.2006.12.006.

Whitson, C. H., Rahmawati, S. D., and Juell, A. 2012. Cyclic Shut-in Eliminates Liquid-

Loading in Gas Wells. Paper presented at the SPE/EAGE European Unconventional Resources Conference and Exhibition, 20-22 March, Vienna, Austria. <http://dx.doi.org/10.2118/153073-MS>.

Yuan, G., Pereyra, E., Sarica, C., and Sutton, R. P. 2013. An Experimental Study on Liquid Loading of Vertical and Deviated Gas Wells. *SPE Production and Operations Symposium*, **3**. <http://dx.doi.org/10.2118/164516-MS>.

Yusuf, R., Veeken, K., and Hu, B. 2010. Investigation of Gas Well Liquid Loading with a Transient Multiphase Flow Model. Paper SPE-128470-MS presented at the SPE Oil and Gas India Conference and Exhibition, 20-22 January, Mumbai, India. <http://dx.doi.org/10.2118/128470-MS>.

Zabaras, G., Menon, R., Schoppa, W., and Wicks III, M. 2013. Large Diameter Riser Laboratory Gas-Lift Tests. Offshore Technology Conference, Houston, TX, 6-9 May.

Zhang, H., Falcone, G., Valko, P. P., and Teodoriu, C. 2009. Numerical Modeling of Fully-Transient Flow in the Near-Wellbore Region during Liquid Loading in Gas Wells. Paper presented at the Latin American and Caribbean Petroleum Engineering Conference, 31 May – 3 June, Cartagena de Indias, Colombia. <http://dx.doi.org/10.2118/122785-MS>.

## Appendix: Permissions to Publish Previously Published Works

The following is a license agreement to publish the article “Modeling Vertical Flow in Churn and Annular Flow Regimes in Small- and Large-Diameter Pipes” in this thesis. The content of this article is split and presented in Chapters 1, 2, 3, 4 and 5.

**Erika Viana Pagan**

---

**From:** Georgia Coomes <gcoomes@bhrgroup.co.uk>  
**Sent:** Wednesday, July 06, 2016 4:45 AM  
**To:** Erika Viana Pagan  
**Subject:** RE: Permission to use content of a paper presented and published at BHR Group's 10th North American Conference on Multiphase Technology 8-10th June 2016

Dear Erika,

Sorry for my delayed response. I have been on annual leave and have since been off work ill. I am checking my emails remotely.

Our copyright terms are;

In consideration for publication of the contribution named above, the undersigned hereby assigns to BHR Group the copyright in the said contribution, whereby BHR Group shall have the exclusive right to publish the contribution and/or translation of it throughout the world during the full term of copyright, including renewals and/or extensions, and all subsidiary rights. The undersigned shall, however, retain the right to republish his/her contribution in any scholarly journal consisting solely of his/her own writings, subject only to notifying BHR Group of his/her intention to do so and to his/her ensuring that the publication by BHR Group is properly credited and that the copyright notices repeated verbatim. The undersigned hereby warrants to BHR Group that his/her contribution has not been published elsewhere or is pending publication elsewhere, or that if it has been published in whole or in part, any permission to publish it has been obtained and provided to BHR Group together with the original copyright notice. BHR Group shall not be responsible for any copyright fees. The paper represents the opinions of the undersigned and BHR Group shall not accept responsibility for any statement made in the paper.

You may of course re-publish your paper, please state where doing so 'Presented and Published at BHR Group's 10th North American Conference on Multiphase Technology 8-10th June 2016'

Kind regards,

Georgia

---

**From:** Erika Viana Pagan [epagan2@lsu.edu]  
**Sent:** 29 June 2016 16:54  
**To:** Georgia Coomes  
**Cc:** Paulo Waltrich  
**Subject:** Permission to use content of a paper presented and published at BHR Group's 10th North American Conference on Multiphase Technology 8-10th June 2016

Dear Georgia,

I am the first author for the paper of title: "Modeling Vertical Flows in Churn and Annular Flow Regimes in Small- and Large-Diameters Pipes" presented at BHR Group's 10th North American Conference on Multiphase Technology 8-10th June 2016 by Paulo Waltrich (who is my advisor for my Master in Science in Petroleum Engineering program)

I would like to ask you permission to use the content of this paper for my Master thesis document. My thesis document will be viewable on the web after accepted by LSU Graduate School.

If you need any other information, please let me know.

I look forward hearing from you soon.

Thank you,

Erika Viana Pagan  
Craft & Hawkins Dept. of Petroleum Engineering  
120 Ingram Hall, Louisiana State University Baton Rouge, LA - 70803 [epagan2@lsu.edu](mailto:epagan2@lsu.edu) | (407) 4516230

The following is a license agreement to publish the article “A Simplified Transient Model to Predict Liquid Loading in Gas Wells” in this thesis. The content of this article is split and presented in Chapters 1, 2, 3, 4 and 5.

5/30/2016	RightsLink Printable License
<b>SOCIETY OF PETROLEUM ENGINEERS LICENSE TERMS AND CONDITIONS</b>	
May 30, 2016	
<hr/>	
<p>This is a License Agreement between Erika Viana Pagan ("You") and Society of Petroleum Engineers ("Society of Petroleum Engineers") provided by Copyright Clearance Center ("CCC"). The license consists of your order details, the terms and conditions provided by Society of Petroleum Engineers, and the payment terms and conditions.</p>	
<p>All payments must be made in full to CCC. For payment instructions, please see information listed at the bottom of this form.</p>	
License Number	3879051328680
License date	May 30, 2016
Licensed content publisher	Society of Petroleum Engineers
Licensed content publication	SPE Proceedings
Licensed content title	A Simplified Transient Model to Predict Liquid Loading in Gas Wells
Licensed content author	Erika V. Pagan, Louisiana State University; Wesley Williams, Louisiana State University; Paulo J. Waltrich, Louisiana State University et al
Licensed content date	2016
Type of Use	Thesis/Dissertation
Requestor type	author of the original work
SPE member	yes
SPE member number	4125508
Format	electronic
Portion	full article
Will you be translating?	no
Distribution	1
Order reference number	05302016
Title of your thesis / dissertation	MODELING CHURN AND ANNULAR FLOW REGIMES IN VERTICAL AND NEAR-VERTICAL PIPES WITH SMALL AND LARGE DIAMETERS
Expected completion date	Aug 2016
Estimated size (number of pages)	82
Total	0.00 USD
Terms and Conditions	
<p><b>STANDARD TERMS AND CONDITIONS FOR REPRODUCTION OF MATERIAL</b></p> <p>1. The Society of Petroleum Engineers, Inc. ("SPE") holds the copyright for this material. By clicking "accept" in connection with completing this licensing transaction, you agree that the following terms and conditions apply to this transaction (along with the Billing and Payment terms and conditions established by Copyright Clearance Center, Inc. ("CCC"), at the time that you opened your RightsLink account and that are available at any time at ).</p>	
<a href="https://is100.copyright.com/AppDispatchServlet">https://is100.copyright.com/AppDispatchServlet</a>	
1/3	



2. SPE hereby grants to you a non-exclusive license to use this material. Licenses are for one-time use only with a maximum distribution equal to the number that you identified in the licensing process; any form of republication must be completed within six months from the date hereof (although copies prepared before then may be distributed thereafter); and any electronic posting is limited to the period identified in the licensing process.
3. You may not alter or modify the material in any manner (except that you may use, within the scope of the license granted, one or more excerpts from the copyrighted material, provided that the process of excerpting does not alter the meaning of the material or in any way reflect negatively on SPE or any writer of the material or their employer), nor may you translate the material into another language.
4. Total excerpts from the license material may not exceed thirty percent (30%) of the total text. Not more than five (5) excerpts, figures, tables, or images may be used from any given paper. Multiple permission requests may not be used to exceed these limits.
5. SPE reserves all rights not specifically granted in the combination of (i) the license details provided by you and accepted in the course of this licensing transaction, (ii) these terms and conditions and (iii) CCC's Billing and Payment terms and conditions.
6. While you may exercise the rights licensed immediately upon issuance of the license at the end of the licensing process for the transaction, provided that you have disclosed complete and accurate details of your proposed use, no license is finally effective unless and until full payment is received from you (either by SPE or by CCC) as provided in CCC's Billing and Payment terms and conditions. If full payment is not received on a timely basis, then any license preliminarily granted shall be deemed automatically revoked and shall be void as if never granted. Further, in the event that you breach any of these terms and conditions or any of CCC's Billing and Payment terms and conditions, the license is automatically revoked and shall be void as if never granted. Use of materials as described in a revoked license, as well as any use of the materials beyond the scope of an unrevoked license, may constitute copyright infringement and SPE reserves the right to take any and all action to protect its copyright in the materials.
7. You must include the appropriate copyright and permission notice and disclaimer in connection with any reproduction of the licensed material. The copyright information is found on the front page of the paper immediately under the title and author. This statement will then be followed with the disclaimer, "Further reproduction prohibited without permission." Examples: 1) Copyright 1990, Society of Petroleum Engineers Inc. Copyright 1990, SPE. Reproduced with permission of SPE. Further reproduction prohibited without permission. 2) Copyright 2010, IADC/SPE Drilling Conference and Exhibition Copyright 2010, IADC/SPE Drilling Conference and Exhibition. Reproduced with permission of SPE. Further reproduction prohibited without permission. 3) Copyright 2008, Offshore Technology Conference Copyright 2008, Offshore Technology Conference. Reproduced with permission of OTC. Further reproduction prohibited without permission. 4) Copyright 2005, International Petroleum Technology Conference Copyright 2005, International Petroleum Technology Conference. Reproduced with permission of IPTC. Further reproduction prohibited without permission. If for any reason, the copyright on the paper is missing or unclear, please follow Example 1 above, using SPE as the default copyright holder. SPE administers copyright for OTC, IPTC and other joint events on behalf of all parties in those events.
8. SPE makes no representations or warranties with respect to the licensed material and adopts on its own behalf the limitations and disclaimers established by CCC on its behalf in its Billing and Payment terms and conditions for this licensing transaction.
9. You hereby indemnify and agree to hold harmless SPE and CCC, and their respective officers, directors, employees and agents, from and against any and all claims arising out of

your use of the licensed material other than as specifically authorized pursuant to this license.

10. This license is personal to you, but may be assigned or transferred by you to a business associate (or to your employer) if you give prompt written notice of the assignment or transfer to SPE. No such assignment or transfer shall relieve you of the obligation to pay the designated license fee on a timely basis (although payment by the identified assignee can fulfill your obligation).

11. This license may not be amended except in a writing signed by both parties (or, in the case of SPE, by CCC on SPE's behalf).

12. SPE hereby objects to any terms contained in any purchase order, acknowledgment, check endorsement or other writing prepared by you, which terms are inconsistent with these terms and conditions or CCC's Billing and Payment terms and conditions. These terms and conditions, together with CCC's Billing and Payment terms and conditions (which are incorporated herein), comprise the entire agreement between you and SPE (and CCC) concerning this licensing transaction. In the event of any conflict between your obligations established by these terms and conditions and those established by CCC's Billing and Payment terms and conditions, these terms and conditions shall control.

13. This Agreement shall be governed and interpreted by the laws of the State of Texas, United States of America. Regardless of the place of performance or otherwise, the Agreement, and all schedules, amendments, modifications, alterations, or supplements thereto, will be governed by the laws of the State of Texas, United States of America. If any provisions of the Agreement are unenforceable under applicable law, the remaining provisions shall continue in full force and effect.

Other Terms and Conditions:

v1.1

Questions? [customercare@copyright.com](mailto:customercare@copyright.com) or +1-855-239-3415 (toll free in the US) or +1-978-646-2777.

### **Vita**

Erika Viana Pagan, a native of Teresina, Piaui, Brazil, received her Bachelor's degree in Chemical Engineering from Universidade Federal do Ceara (UFC). She was accepted into the LSU Petroleum Engineering program where she anticipates graduating with her Master's degree in August 2016.